A Twist of Nature – The Significance of Atropisomers in Biological Systems

Journal:	*Natural Product Reports*
Manuscript ID:	NP-REV-09-2014-000121.R2
Article Type:	Review Article
Date Submitted by the Author:	04-Aug-2015
Complete List of Authors:	Smyth, Jamie; University of Wollongong, School of Chemistry Butler, Nicholas; University of Wollongong, School of Chemistry Keller, Paul; University of Wollongong, Chemistry

NPR

Review

A Twist of Nature – The Significance of Atropisomers in Biological Systems

Received 00th January 20xx,
Accepted 00th January 20xx

DOI: 10.1039/x0xx00000x

www.rsc.org/

Jamie E. Smyth, Nicholas M. Butler, and Paul A. Keller[*†]

Recently identified natural atropisomeric compounds with potential medicinal applications are presented. The ability of natural receptors to possess differential binding between atropisomers is an important factor when considering active and inactive atropisomeric drugs, and has required the development of new techniques for atropselective synthesis of desired targets. Advances in this field therefore have significant relevance to modern pharmaceutical and medicinal chemistry. The atropisomeric natural products discussed include hibarimicinone, flavomannins, talaromannins, viriditoxin, rugulotrosin A, abyssomicin C, marinopyrroles, dixiamycins, streptorubin B, ustiloxins A-F, haouamine A, bisnicalaterines, and tedarene B, all of which show significant potential as leads in antibiotic, antiviral and anticancer studies. The importance for the development of common practices regarding atropisomer recognition and classification is also emphasized.

1 Introduction

Natural products have long been a source of inspiration for medicinal chemists, with a multitude of current pharmaceuticals derived from traditional medicines or biological effectors. Such compounds elicit a targeted and measured response, thus making them an excellent stimulus in the design and synthesis of new therapeutics. The activities of these naturally-produced scaffolds are attributed primarily to the presence of specific functional groups which complement the target site of a protein. However, given the specific tertiary structure of proteins, the geometric orientation of bioactive molecules is crucial to their ability to favourably interact with active and allosteric sites. Thus, an understanding of the relationship between structure and activity is crucial in new drug development, and is of particular importance with respect to chiral compounds.

1.1 Defining Atropisomerism

The most widely documented category of stereoisomerism is that of central, or point, chirality, which generally refers to the geometric arrangement of substituents of a single carbon atom, and is typically designated as either an (*R*) or (*S*) configuration. Point chirality is an inherent feature in all biological systems; a simple and common example being amino acids (excluding glycine), which exist primarily in the levorotatory form. This substantiates the prevalence of stereoisomerism in naturally produced compounds, and the necessity that drug molecules exhibit an ideal geometric orientation for selective interaction with target proteins. While this end is most commonly achieved by control of point chirality, there exists an under-appreciated form of isomerism, which arises from conformational restriction; namely atropisomerism.

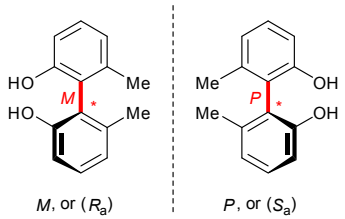

Figure 1: Restricted rotation about a biaryl bond, giving rise to (*M*) and (*P*) atropisomers, with alternate nomenclature of R_a and S_a respectively (subscript a indicating axial chirality), with highest priorities assigned to the *ortho* hydroxyl groups.

Atropisomerism (from the Greek *atropos*, meaning 'not turning') refers to the restricted rotation of a single bond, which effectively locks the configuration into a 'minus' (*M*) or 'plus' (*P*) isomer (Figure **1**), and in many cases may be visualised as a 'helicity'. By definition, atropisomers must be fully resolvable at room temperature for ≥1000 seconds, corresponding to an energy barrier of 23.3 kcal.mol^{-1} – the main distinguishing feature between atropisomers and rotamers.[1] Molecules with significant steric congestion generally have the potential to exhibit atropisomerism, and as such, this phenomenon is most often observed between two *ortho*-substituted aryl systems; however, any forces which are adequate to impose a high enough energy barrier to rotation may give rise to atropisomers, including any attractive or repulsive forces (H-bonding, ionic interactions, π-stacking), or even in strained macrocyclic systems.[2, 3] It is important to note that more than one bond may be hindered to give rise to atropisomerism. Unlike stereogenicity arising from point

[a] School of Chemistry, University of Wollongong, Wollongong, Australia 2522
† Corresponding author: Email: keller@uow.edu.au
See DOI: 10.1039/x0xx00000x

chirality, which may only be altered through the breaking and reformation of chemical bonds, the configuration of atropisomers is governed primarily by their thermodynamic environment. Differing physiological environments within biological systems may therefore provide more specific targets for atropisomeric drugs, as they may be thermodynamically activated or deactivated.

Protein structure is primarily governed by its sequence of amino acid residues, which give rise to intramolecular interactions that govern secondary and tertiary arrangements. As a result of these forces, the active site of a protein is folded into a specific conformation, which may complement a narrow range of substrates. The three-dimensional shape of stereogenic molecules is therefore of particular importance to the ability of an effector to interact with a protein. Thus, atropisomeric molecules may vary in binding specificity and activity, and consequently stereo-controlled syntheses are required in the production of potential pharmaceuticals. The past decade has seen a marked increase in the identification and appreciation of atropisomers as specific drug leads, which has driven the development of new synthetic techniques to allow the stereoselective generation of derivatives.[3]

Given the significance of stereoisomerism and the wealth of molecular structures that natural product chemistry provides, there is a need to highlight the modern emphases in atropisomeric stereochemistry; in particular the requirement for more awareness of its existence, especially in emerging studies on natural products. This review is by no means a comprehensive overview of all natural molecules exhibiting atropisomerism. Rather, the approach has been to provide examples of newly emerging atropisomeric natural products, with a particular emphasis on systems which do not contain the 'traditional' biaryl axis. This being said, several traditional biaryls have been outlined, as they are the most well-studied examples, and offer possible analytical and synthetic insight into all types of conformationally restricted molecules. Although systematically not possible for all examples, this report also provides any additional outcomes reported for these systems, including (but not limited by) synthesis of stereoisomers, biological uses, detection and assignment of stereochemistry, and in a few cases, the biological origins of the molecules. Significant applications also exist for atropisomeric drugs as potential therapeutic agents, and as such, detection and analysis techniques are ever-improving, resulting in a greater understanding of the underlying principles and dynamics which govern these systems.

Therefore, with the growing appreciation of the atropisomeric phenomenon, both in traditional biaryl systems and more modern cases (*e.g.* conformationally restricted macrocycles), presented here are a series of modern reports outlining both intriguing new stereogenic structures, but also advances in knowledge of some perennial examples of atropisomerism, showing that even famous examples are still be investigated with more knowledge surrounding their atropisomerism emerging.

1.2 Natural Atropisomerism in Medicinal Chemistry

There are many well-documented atropisomeric pharmaceuticals, whose utility as effective drugs or leads have been demonstrated, though their axial chirality is often unappreciated. Therefore, it is worth mentioning the almost clichéd example of bioactive atropisomerism, vancomycin – the well-known glycopeptide antibiotic, often used as a drug of last resort for penicillin-resistant bacterial infections. Discovered in 1953, it was found to be produced by soil bacteria, *Amycolatopsis orientalis*, and exhibits broad-spectrum activity against a number of gram-positive bacteria.[4] Less appreciated is that the clinical formulation of vancomycin is exclusively the (*P*) isomer of the molecule (Figure **2**, Compound **1**); the highly-strained cyclophane (*M*) isomer remains undetected.[5] This exclusivity also extends to the axial chirality shown by both biaryl ethers. The increasing instances of vancomycin resistance have hence necessitated the need for alternative treatments, though it is clear that this naturally-produced atropisomer has played a crucial role in the progression of antibiotic drugs, and has acted as a safeguard from penicillin-resistant microbes for decades.[6]

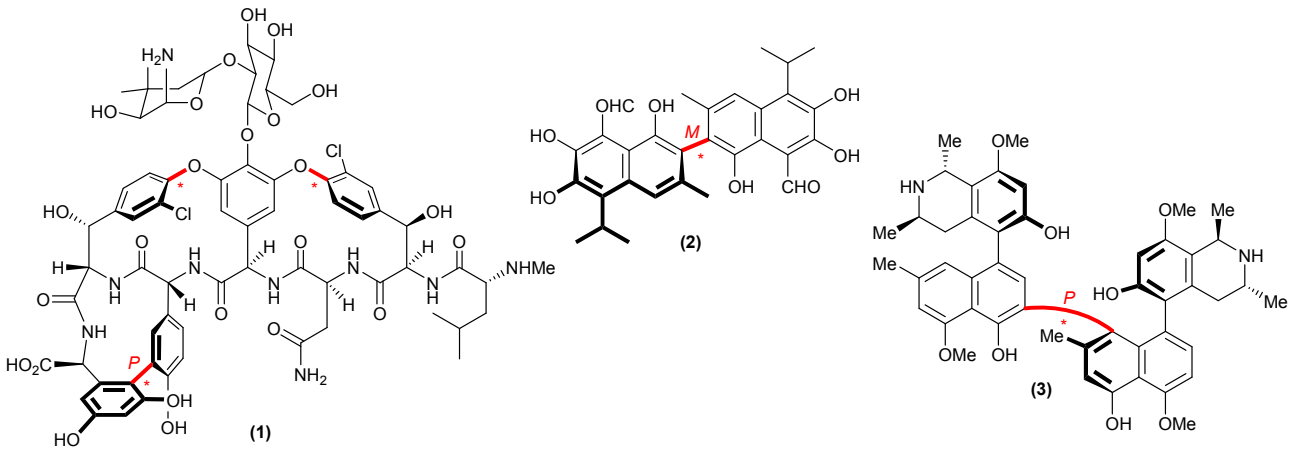

Figure 2: The structure of vancomycin B (**1**), the active (*M*)-gossypol (**2**), and Mbandakamine A (**3**), with chiral axes shown in red.

Another perennial example is the toxic gossypol (Figure **2**, Compound **2**), a compound produced by the *Gossypium* cotton genus, which has been shown to have possible applications as an antifertility and anticancer agent through binding to antiapoptotic protein Bcl-X_L. Even though this is a classic example of natural product biaryl atropisomerism, it has only recently been shown that the active atropisomer of gossypol is that of the (*M*)-(-) enantiomer.[7] This atropisomeric configuration is an order of magnitude more potent than the (*P*)-(+) enantiomer, hence current studies are focussed on identifying plant species which preferentially produce (*M*) over (*P*) with a high enantiomeric excess in an attempt to reduce systemic toxicity. Thus far, the highest observed production was by the *Thespia danis* Oliv. (Malvacea), with a production ratio of 78(*M*):22(*P*).[7] Consequently, a variety of atropisomeric derivatives of the (*M*)-(-)-gossypol scaffold have been synthesized in an attempt to reduce the side-effects of the compound, of which several have shown enhanced activity against Bcl-X_L protein.[8]

The naphthylisoquinoline alkaloids are another important class of atropisomeric natural products worthy of mention in these early stages. These natural products are among the best studied examples of atropisomers, and have been extensively investigated;[9] including their isolation, identification, stereoselective syntheses, biological activities[10] and biosynthetic origin.[11] Here we depict one of the most recent examples reported by the Bringmann group; Mbandakamines A (Figure **2**, Compound **3**) and B (not shown), which are unsymmetrical dimeric alkaloids isolated from an *Ancistrocladus* species collected from the Congo.[12]

In recent years, there has also been a creative appreciation of 'non-traditional' atropisomerism associated with diazepine moieties.[13] Though these molecules themselves do not contain a stereogenic carbon or biaryl axis, they exhibit atropisomerism through conformational inversion of the non-planar ring. The diazepine moiety forms the core of a variety of natural effector molecules; though a variety of synthetic drugs, like benzodiazepine (Figure **3**, Compound **4**), are more widely known. The stereodynamic properties of such compounds are crucial when considering eutomer/distomer relationships for pharmaceutical application, requiring analysis of rotational energy barriers, and hence racemization rates.

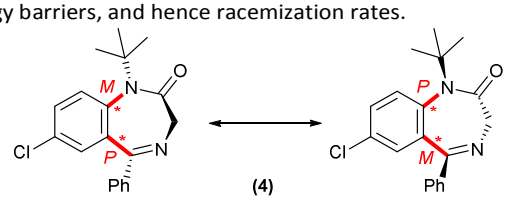

Figure 3: The two possible configurations of benzodiazepine (**4**).

1.3 The Detection of Atropisomerism in Natural Products

Though often overlooked, several procedures exist whereby the absolute configuration around an atropisomeric axis may be determined. Primarily, recognition of atropisomers comes from the identification of motifs particular to them, such as a substituted biaryl moiety. Detection generally relies on the enhanced effect of such molecules on plane-polarized light, usually utilising electronic circular dichroism (ECD) to probe the electronic transitions of UV-active regions, and/or vibrational circular dichroism (VCD) to probe vibrational transitions of the IR-active regions.[14] The ECD/VCD spectra of two atropenantiomers will appear as near-mirror images of each other (i.e. as opposite phases), and as such are relatively simple to distinguish between. However, to determine which spectrum corresponds to a particular configuration requires further analysis; often extensive 2D NMR techniques, however computational prediction is more routine. There are various *ab initio* methods which may be applied,[15] though the most common of these relies on optimizing the structures of the two predicted atropenantiomers with a density functional theory (DFT), then applying a time-dependent (TD) perturbation to predict the vibrational or electronic transitions.[16] Thus, the TD-DFT method calculates CD spectra, which may be compared to experimental spectra to confidently assign the relative atropisomerism. However, a number of shortcomings exist with this method, particularly in that axial chirality dominates the signal of CD spectra, and overwhelms any influence that stereogenic atoms may have on the polarized light; this means that the absolute configuration of such centres must be determined through other methods, such as X-ray crystallography or NOE analysis.[15, 17]

An understanding of the half-lives of atropisomers is also crucial if intended for pharmaceutical use, as one form may have undesirable effect, or may simply be inactive, giving rise to complications in shelf-life and dosage. Generally, such half-lives are determined using chiral HPLC at low temperatures, to evaluate the configurational stability of an atropisomer against inversion, though computational calculation of rotational energy barriers is also an effective technique.

2. Recent Detection and Synthesis of Selected Biaryl Atropisomers in Natural Products

2.1 Hibarimicinone: A microbial intermediate with antitumoral and antibiotic properties

In 1997, the Oki group conducted screening of microbial products for potential protein kinase inhibitors, and found that a strain of *Microbispora rosea*, isolated from soil extracts from the Hibari region of Japan, contained multiple compounds with varying inhibitory activities.[18] Analysis of the microbial cellular debris identified the presence of a new class of compounds, which were referred to as the 'hibarimicins'.

This family of molecules all contain a quasi-dimeric tetracycline backbone, with the variations of hibarimicins A, B, C, D, and G arising from differing carbohydrate substituents (Figure **4**, Compounds **5a**-**5e**). UV-vis analysis, IR spectroscopy, FAB-MS, and exhaustive NMR studies (including COSY, HMBC, and NOE) were used to assign the relative structure of hibarimicin B,[19] and the structures of the other hibarimicins inferred from spectral comparison. Hibarimicinone was determined to be the

aglycon precursor forming the core of the hibarimicins, with the structure of a polyketide with a naphthyl-naphthoquinone structure (Figure **4**, Compound **5f**).

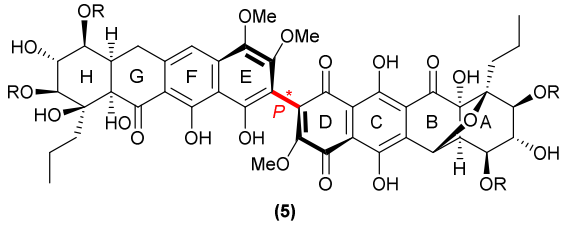

Figure 4: The general structure of the hibarimicin family of molecules; hibarimicins (A, B, C, D, G) R = Sugar (**5a-e**); hibarimicinone R = H (**5f**).

The atropisomerism that the hibarimicin family exhibit arises from restricted rotation about the biaryl axis connecting rings D and E, imposed by the four *ortho* substituents (Figure **4**). To elucidate the absolute configuration around this bond, a C_2-symmetric shunt metabolite HMP-Y6 – a glycosylated structural analogue of hibarimicinone – was synthesized by Romaine *et al,* utilising a biomimetic homocoupling, and two-directional bis-annulation.[20] Using chiral-LC, the racemic mixture was optically resolved into (*M*) and (*P*) components, and using ECD spectra it was observed that the natural products are all exclusively in the (*P*) configuration. Importantly, it was noted that upon heating to 60 °C, hibarimicinone was found to be exclusively in the (*M*) form, indicating the thermodynamic favourability of this *(M)* isomer, and suggesting that the naturally produced *(P)* isomer is a kinetic product.[20]

It was only in recent years that the complex natural metabolite itself was first successfully synthesised by Tatsuta *et al*.[21, 22] The multi-step synthesis (Scheme **1**) proceeds from a pentasubstituted aryl system (**6**) by a stepwise silver-mediated oxidative dimerisation, and subsequent thiolactonisation to give **7**. This is then converted to the axially-chiral scaffold of thiolactone (**8**) by a subsequent kinetic resolution following the installation of a chiral carboxylate system, which was later removed. A dual-Michael–Dieckmann cyclization with the chiral decalin **9** furnished the fused core scaffold **10**, which upon deprotection and intramolecular etherification gave the desired hibarimicinone (**5f**).[21] The final yield of the native (*P*) atropisomer **5f** was 22% from the enantiopure biaryl thiolactone **8**, and could be quantitatively converted to the (*M*) form by heating to 60 °C in neutral methanol.[22] To ensure minimal interconversion between atropisomers during the reaction, the reaction temperature at each step was maintained below 60 °C.

An alternate synthesis was reported in the same year by Liau *et al*, instead utilising an unsymmetrical two-directional double annulation on a racemic mixture of a core biaryl structure (i.e. both *M* and *P* forms), followed by etherification, to generate both atropisomers of **5f** in comparable yields.[23] Importantly, this group determined that interconversion between **5f** and *atrop*-**5f** is more likely pH dependent, as heating in acidified methanol provided little change in atropisomer composition. The group postulated that conversion to the more stable (*M*) form required access to a deprotonated intermediate, facilitated by an environment of pH 7.5, rather than a strictly thermal energy threshold. Examples of natural atropisomerism such as this demonstrate the ability of atropisomers to interconvert between (*M*) & (*P*) isomers, which may prove to be a distinct advantage of atropisomeric systems in exploring active-inactive molecular switching.

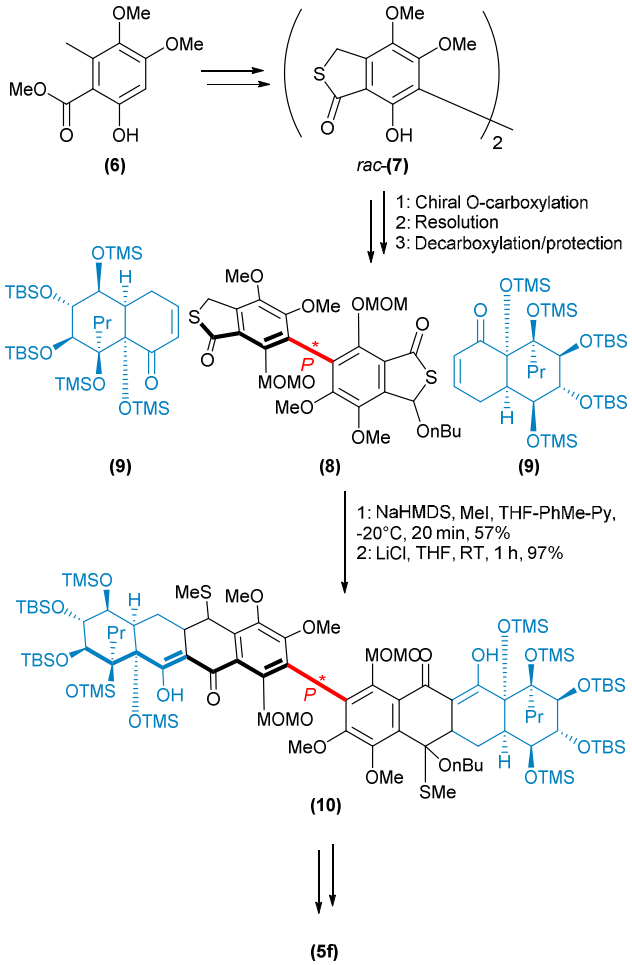

Scheme 1: The first synthesis of hibarimicinone (**5f**), with construction of the hibarimicin core by a dual-Michael-Dieckmann reaction of central thiolactone **8** with **9**, furnishing the final product **5f** after deprotection.

In terms of the biosynthesis of the hibarimicins, it was initially postulated to most likely be produced by a polyketide synthase.[19, 24] Using ^{13}C-labelling and blocked mutants of the TP-A0121 strain, Oki *et al* demonstrated that hibarimicinone is produced *via* an oxidative coupling of a precursor monomer polyketide, which undergoes an oxidative cyclisation to generate the ether ring between cycles A and B, and was identified as the atropisomeric aglycone precursor to the other hibarimicins.[25] There are ongoing studies towards a biomimetic synthesis utilising oxidative dimerization of the hibarimicins, though these have thus far proven unsuccessful.[26]

The extracted compounds (Hibarimicins A, B, C, D and G) were screened for inhibition of calmodulin-dependent protein

kinase III (CAMKIII), protein kinase A (PKA), protein kinase C (PKC), and protein tyrosine kinase (PTK). All of the natural molecules had potent PTK and CAMKIII inhibition, though showing little inhibition of both PKA and PKC, indicating specificity to the PTK protein. MIC values of PTK for the hibarimicins were around 1.8 µM, and 1.2 µM for hibarimicinone, and the hibarimicins also displayed some degree of HL-60 cell differentiation. Further investigation revealed that all of the identified compounds exhibited a mild gram positive antibacterial inhibition, with MIC values ranging from 0.8-12.5 µg/mL.[18] Hibarimicinone was found to be the most potent tyrosine kinase inhibitor, and unlike its derivatives appeared to be a non-competitive inhibitor; however it was also less selective.[27] The success of this synthetic approach allows for the generation of derivatives for drug development, and also provides foundations for the synthesis of other biaryl atropisomers. Hibarimicinone in particular has the potential for specific tyrosine kinase inhibition, though additional studies into potential medicinal application are required.

2.2 Flavomannins and talaromannins: Potential novel route for antibiotic action

The native defences of fungi and bacteria provide a significant resource in the discovery of new antibacterial drugs, due to highly-evolved target specificity and selectivity, which make them attractive prospects. Lesser-investigated sources of bioactive molecules are endophytic fungi that reside within both plants and marine species.[28] It was recently discovered by Bara *et al* that the *Talaromyces wortmannii* fungus, an endosymbiont of Egyptian *Aloe vera* (Asphodeloideae), contained several bioactive atropisomeric compounds; and the group conducted extremely extensive studies to determine any potential medicinal application.[29]

Analysis of the isolated products[26] found that they were similar to that of previously-reported flavomannin,[30] allowing for general structural assignment (Figure **5**, Compounds **11** and **12**). HR-ESI/MS revealed an identical molecular composition for both compounds ($C_{30}H_{26}O_{10}$), and near identical UV absorption maxima.[29] Analysis of ^{1}H and ^{13}C spectra for the pair confirmed they are homodimers of atrochrysone, however HPLC separation resulted in a 3.5 minute difference in retention time of the two products. This suggested that the natural products must differ in either configuration around the biaryl axis, or the arrangement of the stereogenic elements. Four other products extracted had similar NMR spectra, however the complexity of these spectra, and the differing masses obtained from HR-ESI/MS, indicated that these were instead two pairs of asymmetric C7-C7' linked dimers. Further analysis indicated these were heterodimers composed of one atrochrysone unit, and one unit of either an ether derivative of atrochrysone, named flavomannins C and D (Figure **5**, Compounds **13** and **14**), or a unit of emodin (Figure **6**, Compounds **15** and **16**), named talaromannins A and B.

ECD analysis of the compounds resulted in three pairs of almost mirror-image spectra, suggesting they are atropdiastereomers. Given that the $[\alpha]_D$ of one of the compounds matched the value previously reported for flavomannin A (**11**),[30] the corresponding compound was thought to be its atropdiastereomer, and dubbed flavomannin B (**12**). Using TD-DFT (B3LYP, BH&HLYP, PBE0/TZVP) ECD calculation protocols, the simulated ECD spectra of both atropisomeric configurations matched well with the experimental ECD data, assuming identical point chirality at C3/C3'. Thus, it was concluded that flavomannin A is the (*M*) atropisomer (**11**), and flavomannin B is the (*P*) atropdiastereomer (**12**).[29] Using the same techniques, the axial chirality of **13** and **14** were assigned as (*P*) and (*M*), respectively; inverted in relation to **11** and **12**, as the addition of the methoxy to the C6' alters the CIP priority assignment. Talaromannins A (**15**) and B (**16**) were also determined to be the (*M*) and (*P*) atropdiastereomers, respectively. However, as previously mentioned, axially-chiral groups such as the biaryl bond dominate the ECD spectrum, and so the absolute configuration of the stereogenic C3' was unable to be conclusively determined. Previously, vibrational circular dichroism (VCD) and vibrational absorption (VA) techniques were successful in the identification of point chirality in the atropisomeric cephalochromin.[31] This method relies on differences between both the calculated VCD and VA of the (*M*) and (*P*) diastereomers, such that by subtracting one from the other, the individual contribution of stereogenic atoms may be determined. However, in this case, the residual signal was negligible, and so no conclusive definitions of absolute configuration of the other stereogenic elements could be drawn.

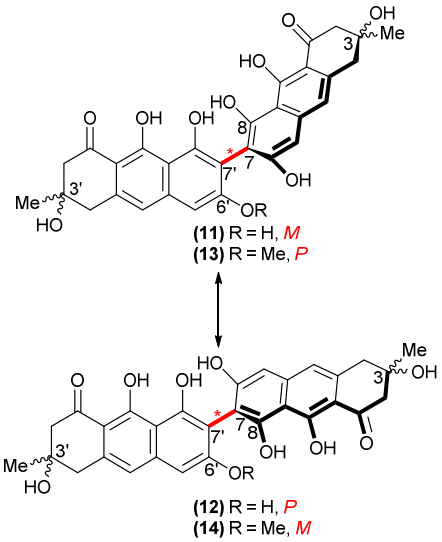

Figure 5: The determined structures of flavomannin A (**11**), flavomannin B (**12**), flavomannin C (**13**), and flavomannin D (**14**), with undetermined point chirality at C3 and C3'. **11** and **12** are homodimers comprised of two atrochrysone moieties connected *via* the atropisomeric bond; wheras **13** and **14** are heterodimers comprised of an atrochrysone moiety (right of atropisomeric bond) and an ether derivative of atrochrysone (left of atropisomeric bond).

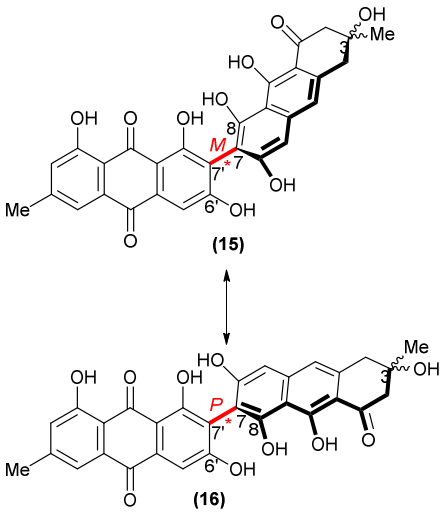

Figure 6: The determined structures of talaromannin A (**15**), and talaromannin B (**16**), with unknown point chirality of C3. The heterodimer is comprised of an emodin moiety (left of atropisomeric bond) and atrochrysone moiety (right of atropisomeric bond).

Currently, there are no reported syntheses for these specific natural products, though it is evident that an atropselective biaryl coupling utilising one of the many well-established techniques (see review by Bringmann *et al*)[3] may be applied to such an end. The biosynthesis of these dimeric compounds also remains ambiguous; though related dihydroanthracenones have been reported for higher order plants, the pathways involved for fungal production may differ significantly, and so cannot be subjected to speculation.

Potential antibacterial activity was determined by subjecting an array of both gram-positive and gram-negative bacteria to each compound, with the highest MIC values (4-8 μg.mL^{-1} for the most potent) observed against *Staphylococci*. Intriguingly, inhibitory data indicates greater effectiveness against multi-resistant strains of *Staphylococci* versus susceptible reference strains. Further investigation into the antibiotic action of the potential atropisomer concluded a bacteriostatic mode of action up to 16 μg.mL^{-1}, and while bactericidal action may be observed at higher concentrations, the hydrophobicity of each of the compounds prevented testing to this end. This antibacterial activity may rely on the C7-C7' axis connecting the two units; recently detected C7-C5' linked regioisomers of flavomannins C and D have proven to have no parallel antibiotic activity.[32] The cytotoxicity of all six atropisomeric natural compounds was tested using THP-1 human leukemic monocyte cells and BALB/3T3 mouse embryonic fibroblast cells, and the IC_{50} values of all were found to be >32 μg.mL^{-1}. These values indicate minimal interference with eukaryotic cell growth and function at therapeutic dosages, indicating potential for specific antibiotic application.

Studies were conducted to elucidate the mode of action of these derivatives using *B. subtilis*, and though no MIC values were found up to 64 μg.mL^{-1}, a reduction in growth rate was observed. Reporter genes in *B. subtilis* were used to determine the pathway affected by the compounds, and it was found that the *yorB* promoter and RecA protein were both induced; indicative of direct interference with DNA structure, synthesis or processing.[33, 34] It was also observed that only the atropisomeric products with negative $\omega_{C6',C7',C7,C8}$ dihedral angles, namely **12**, **14**, and **16**, exhibited induction of these proteins. Additionally, phenotypic analysis of cells treated with **12**, **14**, and **16** showed elongated rod-like cells; an indicator for the induction of the bacterial SOS pathway in response to DNA interference. However, due to the fact that all compounds (**11**-**16**) showed a reduction in *B. subtilis* growth, it was assumed that this was just one pathway through which inhibition occurred, and was reliant on the absolute configuration of the atropdiastereomers. This is promising as it evidences variable activity of therapeutic compounds based on their atropisomeric configuration, however the group concluded it is likely the natural products may have an additional, potentially novel, mode of action though this requires further investigation.

2.3 Viriditoxin: Inhibition of the FtsZ protein and disruption of membrane proteins in bacteria

Bacteria, which lack eukaryotic β-tubulin, utilise a homolog known as FtsZ during replication and division, which polymerizes to form the contractile ring during the initiation of cell division.[35] Thus, FtsZ represents a prime target for specific bacterial inhibition to prevent replication, while eliciting minimal adverse effects to the eukaryotic host. It was during a high-throughput screening for such an inhibitor that the utility of the otherwise 'toxic' viriditoxin was first appreciated.[36]

Viriditoxin was first discovered from extracts of *Aspergillus veridinutans* in 1971, though has since been identified as a component of a number of fungal extracts.[37, 38] The initial structural assignment of viriditoxin by Lillehoj *et al* indicated the structure to be that of an 8,8'-binaphtho-α-pyrone with unassigned stereochemistry, however this structure was revised in 1990 by Kawai *et al*, after NOE spectroscopic analysis revealed the 6,6'-binaphtho-α-pyrone scaffold, and CD analysis revealed the natural atropisomeric configuration of the biaryl axis was exclusively (*M*) (Figure **7**, Compound **17**).[38]

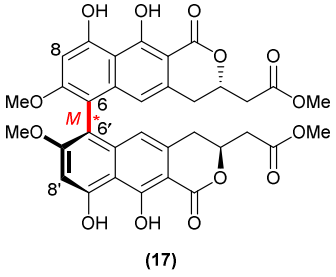

Figure 7: The confirmed structure of the naturally produced (*M*)-viriditoxin (**17**).

Despite this structural assignment, there was little synthetic development of (*M*)-(-)-viriditoxin until recently, when in 2011 Shaw *et al* successfully developed a preparative-scale, atropselective total synthesis, utilising a chiral μ-oxo-divanadium(V) complex to define the stereochemistry about the biaryl axis (Scheme **2**).[39] This initial publication however was quickly succeeded by a second-generation synthesis by

the same group in 2012, reporting improved scalability, yields and atropselectivity.[40] Principally, the synthesis of the necessary precursor to monomer **18** (Scheme **2**) was made simpler by the elimination of large-scale tin-allylation, ozonolysis and LDA-induced cyclisation steps in favour of a strategy which instead utilised aspartic acid as a chiral pool precursor, the formation and ring-opening of a chiral oxirane with a vinyl Grignard reagent, and ring-closing metathesis. Additionally, the use of a larger silyl protecting group (OTBDPS, in place of OTIPS) assisted with stability and stereoselectivity (ratio of >95(*M*):5(*P*) [TBDPS], compared with 89(*M*):11(*P*) [TIPS]) upon dimerisation.

Monomer **18** was prepared by a Michael-Dieckmann strategy, using LDA in DMPU, and subsequent DDQ-mediated aromatisation. The resulting ethoxymethyl-protected phenol was then *O*-methylated, and the protecting group removed using $ZnBr_2$ and *n*-propanethiol. Vanadium-catalyzed oxidative homocoupling of **18** using the novel dimetallic vanadium catalyst **19** in an O_2 atmosphere afforded the desired atropisomeric precursor of (*M*)-viriditoxin with high atropselectivity (ratio of >95(*M*):5(*P*)), and in yields of up to 87% using complex **19**.[39, 40] Final deprotection, oxidation of the alcohol terminus, and esterification furnished (*M*)-viriditoxin (**17**), confirmed by comparison of the optical rotation and NMR spectra of synthesised **17** with those of a genuine sample.[39] The achievement of the synthesis of (*M*)-viriditoxin has allowed for investigations into possible medicinal applications, and importantly, it has also provided a new method with which to control the atropisomerism involving relatively complex molecules with similar binaphthopyranone structures.[39, 40]

Subsequent to the initial studies of its cytotoxicity (LD_{50} 2.8 $mg.kg^{-1}$, mouse) and activation of rat ATPase,[37, 41] there was little more known about the bioactivity of viriditoxin until 2013, when Foss *et al* reported an MIC value of 0.63 µM against *B. subtillus* strain 168, and determined its mechanism of action. Flow cytometry and microscopy undertaken by this group identified that, among other previously identified 'FtsZ inhibitors', viriditoxin acts by dissipating the membrane potential of bacteria, and increasing membrane permeability; not through specific *in vivo* FtsZ inhibition.[42] Both of these factors mean that neither FtsZ nor the key division protein MinD can bind effectively to the membrane, hence halting replication of the bacteria. As such, viriditoxin has been implicated in having significant antibiotic activity towards fish pathogens, which could prove useful in conservation and agricultural fields.[43] In addition to its antibiotic effects, viriditoxin has also shown promise in oncological studies, displaying significant promotion of apoptosis and autophagy in human prostate cancer cells.[44]

2.4 Rugulotrosin A: Further antibiotics from the *Penicillium* genus

In 2004, an extensive screening of Australian fungal and bacterial metabolites by Stewart et al revealed a species of the Penicillium fungus genus (assigned MST-F8741) contained a dimeric tetrahydroxanthone with antibiotic activity; rugulotrosin A (Figure **8**, Compound **20**).[45] Analysis of the NMR data suggested that it was a symmetric dimer about the C2-C2' axis. X-ray crystallography analysis of rugulotrosin A determined the relative configuration of the chiral axis; however the data was insufficient to definitively assign the stereogenic carbons (C6, C7, C6' and C7'), though they were determined to have a relative cis arrangement. The absolute stereochemistry was later determined in a more recent and extensive synthetic study by Qin et al, which permitted access to both atropisomers and enantiomers of rugulotrosin A.

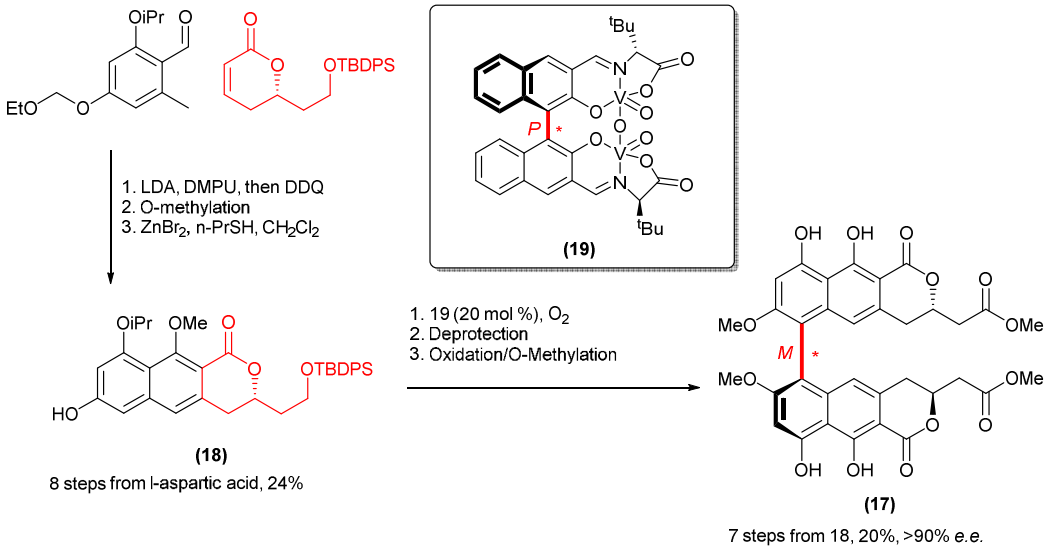

Scheme 2: Synthetic route for the atropselective synthesis of (*M*)-viriditoxin (**17**), utilising a dimetallic atropisomeric vanadium(V) catalyst (**19**) for the dimerization of the naphthopyranone monomer **18**.

NPR

Review

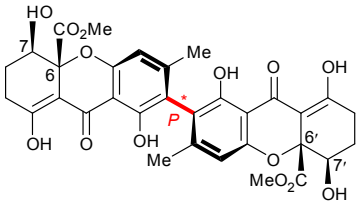

(20)

Figure 8: The determined absolute stereochemistry of naturally produced rugulotrosin A (**20**).

Comparison of CD spectra from the synthesized ±(*M*) and ±(*P*) forms of **20** indicated the natural product was exclusively (6*R*,6'*R*,7*R*,7'*R*) with regards to the stereogenic carbons, with (*P*) axial chirality.[46] A B3LYP/6-31G(d) level of theory calculated a barrier of rotation of 47.7 kcal.mol^{-1} for **20**; the fact no (*M*) atropisomer was observed following heating of **20** in toluene up to 150 °C for 3 h indicates the thermodynamic stability of the (*P*) conformation.[46]

For the aforementioned atropselective synthesis of **20**, Qin. *et al* devised a strategy utilising an achiral ligand in a palladium coupling of two monomer units to elicit a point-to-axial chirality transfer effect. As such, with synthesized iodide **21** in hand, a one-pot Suzuki dimerization in the presence of achiral ligand SPhos generated protected intermediate **22** in 36% yield with diastereomeric ratio of 75(*P*):25(*M*). These were separated by recrystallization, followed by deprotection in 3 M HCl/MeOH, affording both rugulotrosin A and *atrop*-rugulotrosin A in 85% each (Scheme **3**). The group also used HPLC with photodiode array detection (DAD) and ESI-MS to determine that *atrop*-rugulotrosin A is not naturally produced even in trace amounts by *Penicillium* (MST-F8741), indicating the process must be highly atropselective; though no further biosynthetic studies have currently been reported.

Rugulotrosin A has exhibited activities against Gram-positive bacteria, with IC_{50} values of 2.1 µM for *B. subtilis* (ATCC 6633) and 6 µM for *S. aureus* (ATCC 25923); though no activity against the Gram-negative *E. coli* (ATCC 25922) or human lung (NCI-H460) and colon (SW620) cancer cells.[46] Intriguingly, *atrop*-rugulotrosin A had far weaker activity; only notable for an IC_{50} of 10 µM against *B. subtilis* (ATCC 6633). Thus, these natural products are an important example of how atropisomeric configuration can drastically influence the bioactivity of a molecule.

3. Non-Traditional Atropisomerism in Natural Products

As part of improving the recognition of the phenomenon of axial chirality, it is important to note that there are multitudes of various non-traditional (i.e. non-biaryl) systems in which atropisomerism can exist. Many such systems are strained macrocycles, however any instance of hindered rotation about a bond must be acknowledged as having the potential to produce distinguishable atropisomers; hence, a variety of these 'exotic' instances of atropisomerism have been outlined. Also, for these systems, defining the stereochemistry often uses the terminology of *syn*/*anti* or *cisoid*/*transoid*, for convenience in efficiently indicating configuration.

3.1 Abyssomicin C: A promising antibacterial for Tuberculosis

Atropisomerism of an unusual nature was identified when the molecule abyssomicin C was discovered during the pursuit for viable inhibitors of enzymes involved in the *p*-aminobenzoic acid (PABA) synthesis pathway, specifically to treat tuberculosis. PABA is essential for the production of dihydropteroate in bacteria, a precursor for folate formation.[47]

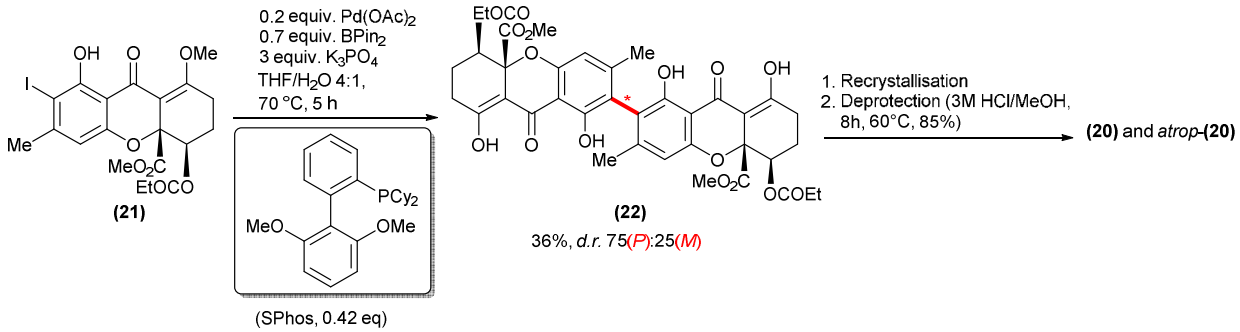

Scheme 3: Atropselective synthesis of rugulotrosin A (**20**) and *atrop*-rugulotrosin A by Qin *et al*. This approach utilises point-to-axial transfer using an achiral ligand during a one-pot Suzuki coupling of monomer 21 to generate protected dimer **22** in 36%, with a d.r. of 75(*P*):25(*M*). These intermediates were separated using recrystallization, and following deprotection afforded rugulotrosin A and *atrop*-rugulotrosin A in 85% each.

NPR

Review

Folate cofactors are vital for the survival of all organisms, and eukaryotes have developed cellular transporters which allow for the importation of folate from dietary sources. Bacteria, however, lack these transporters, and so must synthesize it themselves; making this synthesis pathway an ideal target for direct and specific inhibition. Abyssomicin C itself has already been comprehensively reviewed by Zask *et al* and Savic, however its unique atropisomerism necessitates a brief mention here, in the pursuit of expanding recognition of this phenomenon in non-classical systems.[48, 49]

There were no known inhibitors for this stage of folate synthesis when abyssomicin C was first discovered, hence an assay was devised to screen for any natural compounds which may exhibit activity. Of the actinomycetes screened, only the extracts of *Verrucosispora maris* strain AB-18-032 showed activity.[47] Following chromatographic separation, mass spectral analysis, 1D/2D NMR techniques, and X-ray crystallography were sufficient for the determination of the absolute structure of abyssomicin C (Figure **9**, Compound **23**).[47] The atropisomeric potential for this natural product was not initially recognised until the second successful total synthesis in 2006 by Nicolaou and Harrison (for first synthesis, see Zapf *et al*)[50], which produced both abyssomicin C (**23**) and atrop-abyssomicin C (Figure **9**, Compound **24**).[51] X-ray crystallography of the two revealed their atropdiastereomeric relationship, and the absolute configuration was confirmed; **23** appeared to have a more *transoid* conformation between the C7 carbonyl and C8/C9 double bond (dihedral angle 144.8° O=C7–C8=C9), whereas **24** was found to exist in a more *cisoid* conformation (dihedral angle 26.4° O=C7–C8=C9). It was observed that the isomerism arises from the highly strained eleven-membered ring, and that **24** could not be converted to **23** with heating up to 180°C (xylene, microwave irradiation), requiring instead mildly acidic conditions for conversion at RT (2:1 ratio of **23**/**24**). It was later realised that **24** is in fact the main abyssomicin product of *V. maris* AB-18-032, and that **23** is only a minor product.[52]

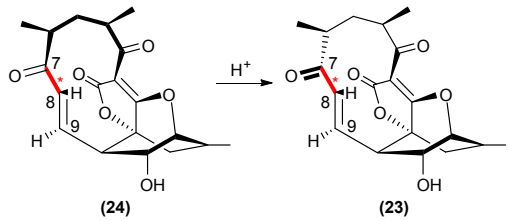

Figure 9: The absolute configuration of abyssomicin C (**23**) and atrop-abyssomicin C (**24**), which may convert to **23** under mild acidic conditions.

This convergent synthesis relied firstly on the generation of a TES-protected oxabicyclo[2.2.2]octane spirotetronate intermediate (Scheme **4**, Compound **25**), which was then elaborated over 6 steps to form intermediate **27** in 38% yield. This was subjected to ring closing metathesis, chemoselective oxidation – assumedly where the atropisomerism of the final product is defined, though this configuration could not be elucidated – and deprotection to yield **24** in 21% over 3 steps from **27**. Though concise and relatively high yielding, this synthetic approach has since been paralleled or superseded by alternate strategies;[53] notably Bihelovic and Saicic's approach, which avoids epoxide ring opening of the tetronate in the hope of higher tolerance in the generation of analogues for SAR studies.[54-56]

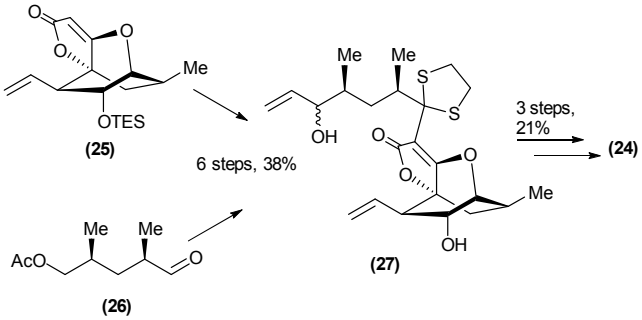

Scheme 4: Convergent synthesis of atrop-abyssomicin (**24**) via connection of spirotetronate intermediate **25** with aldehyde **26** over 6 steps to give **27,** which is subjected to ring closing metathesis, oxidation and final deprotection to give **24**.

In 2011, Gottardi *et al* treated cultures of *V. maris* AB-18-032 with ^{13}C-labelled precursors and found that abyssomicin C is biosynthetically produced from five acetates, two propionates, and a glycolytic pathway metabolite.[57] In the same study, whole genome sequencing and bioinformatical analysis was used to identify genes encoding for proteins related to abyssomicin C biosynthesis, with in-frame deletions of the genes used to confirm their role. Comparison with other biosynthetic studies of tetronate antibiotics aided in the identification of genes responsible for abyssomicin C biosynthesis; three genes encoding for proteins for the generation of the polyketide backbone (which effectively forms the macrocycle in abyssomicin C); five genes encoding for proteins involved in the generation of the tetronate moiety; three genes for further oxidative enzymes; and a variety of other genes related to import, export and packaging of the molecule.[57]

It was noted that the structure of **23** and **24** were similar to that of chorismate, a precursor to PABA,[58] and studies revealed that atrop-abyssomicin irreversibly binds the Cys263 of *E. coli* 4-amino-4-deoxychorismate in a Michael addition,

forming a sulphur-bound abyssomicin D in the process.[47] This mechanism is attributed to the α,β-unsaturated ketone, which is not present in other detected abyssomicins.[59] Higher activity against methicillin-resistant *Staphylococcus aureus* (MRSA) observed for **24** (MIC 3.5 μg.mL^{-1}) over **23** (MIC 5.2 μg.mL^{-1}) has been proposed to arise from differing configurations of the reactive α,β-unsaturated ketone, located either side of the atropisomeric bond.[51] The *cisoid* configuration of the C7 carbonyl relative to the C8/C9 double bond in **24** (i.e. forcing the electron rich systems closer) may increase the conjugation and hence reactivity of this compound relative to its atropdiastereomer. Activities against *Mycobacterium bovis, Mycobacterium smegmatis* and *Mycobacterium tuberculosis* have also been reported,[60] however cytotoxicity against both HeLa and normal somatic cells for several derivatives of abyssomicin C was observed.[54] The recently generated atrop-*O*-benzyl-desmethylabyssomicin C derivative shows decreased cytotoxicity while maintaining antibacterial strength, and may therefore have future medicinal applications.[55]

3.2 Marinopyrroles: Determination of enzymatically-imposed atropselectivity

The omnipresent threat of bacterial resistance necessitates the exploration of novel sources for antibiotic agents; a growing portion of which originate from the under-utilized marine environment. In recent years, the marinopyrrole family of molecules have attracted significant attention, and have already been reviewed extensively,[61, 62] however the intriguing structure of these compounds warrants their mention in this overview of natural atropisomers. In 2008, Hughes C. *et al* isolated two metabolites from *Streptomyces* strain CNQ-418 (found in sediment near La Jolla, California) with a *N,C2*-linked bipyrrole structure (previously unobserved naturally), which were subsequently named marinopyrroles A and B (Figure **10**, Compounds **28** and **29**).[63] Initial attempts at structural elucidation were attempted using 2D NMR techniques, however these proved inconclusive. As such, X-ray crystallographic analysis of marinopyrrole B (**29**) allowed the assignment of absolute structure, and through comparison of similar CD spectral data between **29** and **28**, the structure of marinopyrrole A was inferred.[63] The exclusive *M*-configuration was determined given the X-ray Flack parameter 0.03 obtained for **29**; which showed high likelihood of an *M* configuration about the salicyloyl moieties. In addition to **28** and **29**, marinopyrroles C-F (not shown) were later detected, of which C-E were isolated as exclusively the *M* atropisomer, while marinopyrrole F was extracted as a racemic mixture.

In order to further probe the activity of the marinopyrroles, and to generate a variety of derivatives, various synthetic approaches have been constructed.[61, 64-69] In all cases, these produced racemic mixtures of **28** and **29**, and at this stage no atropselective synthesis has been reported. Of these, the convergent and high yielding synthesis of **28** was achieved by Kanakis and Sarli, who managed to make use of a previously unsuccessful Ullman coupling to establish the bipyrrole core under microwave-assisted conditions, utilising substrates

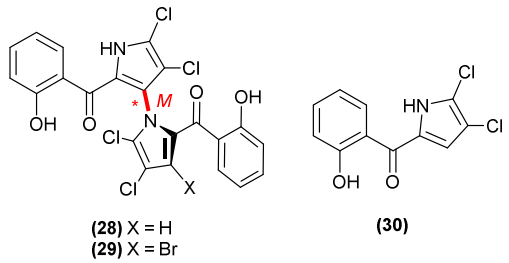

Figure 10: The absolute structures of marinopyrroles A (**28**) and B (**29**), with their composite monomeric precursor monodeoxypyoluteorin (**30**).

containing no halogens other than the bromine necessary for the coupling (Scheme **5**, Compounds **31** and **32**).[68] This afforded *rac*-**28** in 36% yield over 3 steps from the synthesized monomeric units. Various manipulations to **28** and some of its synthetic precursors have allowed access to multiple analogues for SAR studies.[64, 65, 69, 70] The first, and thus far only, synthesis of marinopyrrole B (**29**) was reported in 2013 by Cheng *et al* (not shown), whereby the bipyrrole core in this case was instead generated through alkylation of a trihalogenated pyrrole, which underwent further manipulations to complete a Paal-Knorr construction of the second pyrrole ring, a precursor which allowed for the generation of *rac*-**29**.[71]

The postulated monomeric precursor monodeoxypyoluteorin (Figure **10**, Compound **30**) was also isolated by Yamanaka *et al*, prompting further investigation of the biosynthetic pathway of the marinopyrroles, impressive both for its unprecedented enzymatic bipyrrole homocoupling, and the high degree of atropselectivity with which this aryl coupling occurs.[72] Through appreciation of the similarities between **30** and two closely related phenylpyrrole antibiotics, pyoluteorin and pyrrolomycin D, and based on previous biosynthetic studies for these two compounds, Yamanaka *et al* managed to clone, sequence and isolate the gene cluster responsible for the production of the marinopyrroles into a minimized cosmid. The marinopyrrole biosynthetic genes, *mpy1-16*, were tested for their *in vivo* activities using a *Streptomyces coelicolor* M512 expression system. Through gene deletion, and analysis of **28** production *via* HPLC, it was determined that two genes, *mpy10* and *mpy11*, both encoding $FADH_2$-dependent halogenases, are

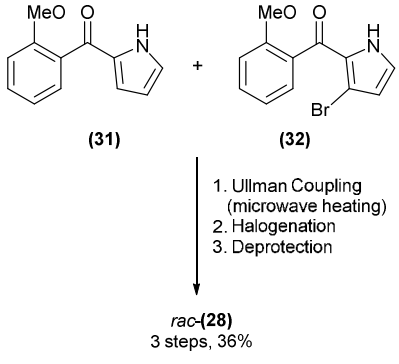

Scheme 5: Convergent total synthesis of racemic marinopyrrole A (**28**).

required for the bipyrrole homocoupling. It was also found that the *mpy12-14* ABC transporter gene cassette was also necessary for marinopyrrole production, assumedly for transmembrane transport of the molecules. Given the two tandem $FADH_2$-dependent halogenase genes *mpy10* and *mpy11* were analogous to two found in the pyrrolomycin D synthesis gene, it was postulated that **30** undergoes C-3 halogenation, followed by enzymatic coupling to another non-halogenated **30** (Scheme **6**, Route **A**). Yamanaka *et al* also proposed that halogenation of the pyrrole nitrogen in **30** could enable electrophilic aromatic substitution in a similar manner (Scheme **6**, Route B). Given a distinct lack of detectable halogenated intermediates, the group concluded that these remain complexed with the protein until the subsequent coupling has taken place.

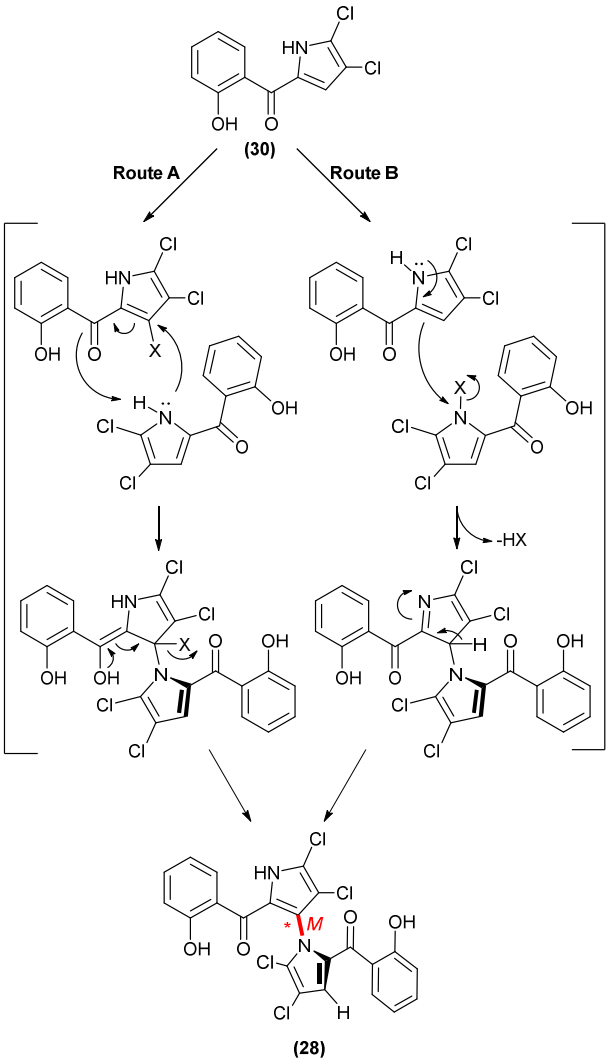

Scheme 6: Proposed mechanisms for the enzymatic synthesis of marinopyrrole A, utilising either (**Route A**) *C*-halogenation and nucleophilic substitution, or (**Route B**) *N*-halogenation and electrophilic substitution. For both cases, X = a halogen (Cl, Br, I)

There has been an array of reports for both antibiotic and antitumor activities of the marinopyrroles and their analogues, and in all studies, very little variation of activity between the *M* and *P* atropisomers was observed. Initial studies showed **28** and **29** had relatively low MIC_{90} values against methicillin resistant *S. aureus*, and exhibited cytotoxic effects on HTC-116, a human colon cancer cell line.[63] Further investigation showed (*M*)-**28** had inhibitory activity against a wide range of MRSA strains and other gram-positive bacteria, as well as against the gram-negative *Haemophilus influenza*.[73] However, it was found that the therapeutic window for **28** is possibly too narrow for effective treatment, and that it is inactivated by human serum, thus potentially only be applicable *in vivo* as a topical agent.[73] That marinopyrrole A has shown a high affinity for binding to plastic indicates a potential use as a medical instrument coating agent to prevent infection, with the added bonus of lowered systemic toxicity from the aforementioned serum inactivation.[61] However, chlorinated and fluorinated derivatives have been generated exhibiting comparable MRSA inhibition and some resistance to serum inactivation, and thus may have future applications.[69] Currently, the main focus of these compounds is the generation of derivatives for anticancer applications. Marinopyrrole derivatives with a cyclic structure and sulphide substituents have proven to be promising inhibitors of the interactions between pro-apoptotic proteins, Bcl-x_L and Mcl-1, and their target pro-survival protein, Bim.[64, 65, 74] It was also found that marinopyrrole A may restore activity of the anticancer drug ABT-737 to resistant cancer cells.[75] As such, these atropisomeric natural products show promise for broad medicinal application, and studies as to this potential are ongoing.

3.3 Dixiamycins: Atropisomeric N-C and N-N coupled dimers from marine actinomyces

During characterisation of metabolites from marine *Streptomyces*, Zhang *et al* re-isolated the previously discovered xiamycin A (Figure **11**, Compound **33**), alongside a series of novel N-C and N-N linked xiamycin dimers,[76] compounds also detected in parallel studies by Hertweck *et al*.[77-79] Though atropisomeric N-N axes have been observed between sp^2-hybridized nitrogen atoms in synthetic studies,[80] this discovery marked the first incidence of a naturally-occurring atropdiastereomeric N-N axis between sp^3-hybridized carbazole nitrogens. The formulae of two atropdiastereomeric compounds were determined to be $C_{46}H_{48}N_2O_6$ using HR-FAB/MS (high-resolution fast atom bombardment), corresponding to a dimer of xiamycin A. The NMR spectra were also similar between the atropisomeric dimers and the monomer, however the lack of an NH signal in the ^1H NMR spectra implied the presence of two N-N coupled dimers, allowing for general structural assignment (Figure **11**, Compounds **34** and **35**).

To calculate the inversion rates of **34** and **35**, preliminary torsion angle scans were used, and the two lower-energy maxima for the global scan were used as the starting geometries for transition state calculations. The rotational energy barriers of **34** and **35** were found to be 199 $kJ.mol^{-1}$ and 201 $kJ.mol^{-1}$ respectively, consistent with experimental data

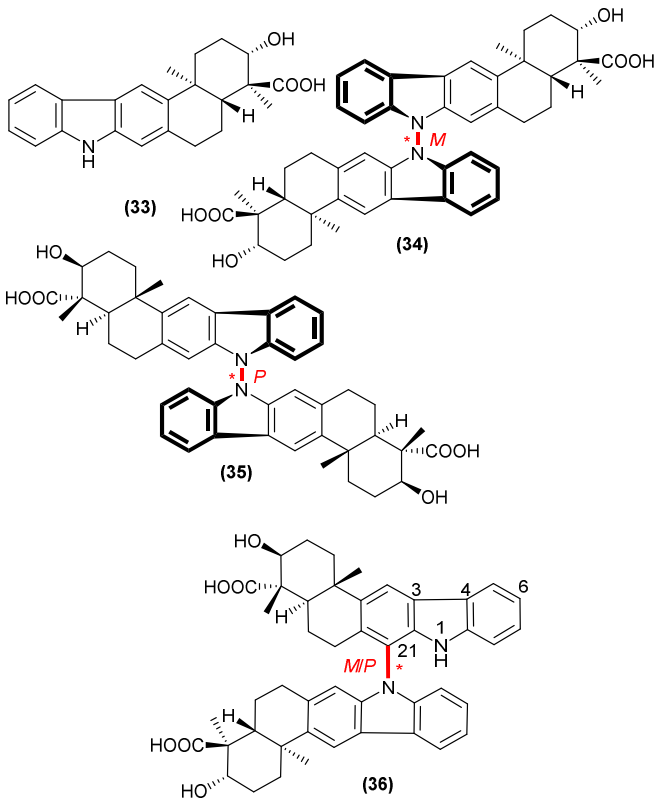

Figure 11: The known structure of xiamycin A (**33**), and determined structures of dixiamycin A (**34**) dixiamycin B (**35**), and an unnamed C-N linked xiamycin dimer (**36**), of which both the *M* and *P* isomers were isolated.

showing thermal interconversion of the two could not be achieved even by heating at 100 °C for 1 hour.[76] These extremely-stable atropdiastereomers were subjected to ECD to determine absolute configuration, a technique which is effective for C-C atropisomeric bonds. However, the two spectra did not appear as the expected mirror-images of each other; instead they were both similar to the ECD of **33**, a phenomenon attributed to the symmetry of the 9-carbazole, the orientation of which is similar between **34** and **35**. The main difference between the two was an intense absorption at 297 nm in **35**, which was absent in **34**. Assuming identical point chirality of the two dimers to the corresponding monomer, **33**, TD-DFT ECD calculations were conducted for both. The resulting spectra displayed that an (*M*) configuration did not yield the observed shoulder at 297 nm, and matched reasonably well with the ECD spectrum found for **34**, which was dubbed dixiamycin A. Calculations for the (*P*) configuration did yield a similar peak at 297 nm, and was attributed to **35**, which was subsequently named dixiamycin B.

Concurrently, studies by Hertweck *et al* revealed a number of N-C linked xiamycin dimers from bacterial extracts, including an unnamed xiamycin dimer (**36**), bearing a C_{21}-N linkage, and a non-atropisomeric structural isomer (dixiamycin C, not pictured) bearing a C_6-N linkage.[78] Analysis of the ^{1}H-NMR spectrum of the unnamed dimer revealed it to be asymmetric by the presence of two sets of peaks, resulting in a total of eleven aromatic protons. The absence of a H_{21} peak and the presence of a peak corresponding to H_{21}' suggested a C-N linkage at C_{21}, which was further supported by ^{1}H-COSY and HMBC experiments. The absolute stereochemistry about the axis was determined for each compound by comparison of experimental CD spectra with a generated TD-CAM-B3LYP/6-31G*//B97D/TZVP spectrum. Conversely, the structure of dixiamycin C, bearing a C-N linkage was determined by ^{1}H-COSY and HMBC experiments, however it was found to be non-atropisomeric.

The first synthesis of dixiamycin A (**34**) was established by Zhang *et al*, by a $KMnO_4$-mediated oxidative coupling N-N indole coupling of xiamycin A (**33**), of which **34** was selectively generated in trace quantities, with no **35** apparent.[76] More recently, Baran *et al* reported a formal total synthesis of dixiamycin B (**35**) and its precursor xiamycin A (**33**), by the development and utilisation of a novel and highly chemoselective electrochemical oxidative N-N coupling.[81] **33** was prepared on gram-scale over nine steps, in an overall 17% yield from chiral oxirane **37**, which was electrochemically oxidised to afford exclusively dixiamycin B in 28% yield, in addition to a brominated xiamycin monomer in 17% yield, and recovered starting material (13%) (Scheme **7**). The reason for the atropselectivity of this reaction is currently not known, and is complementary to that reported by Zhang.

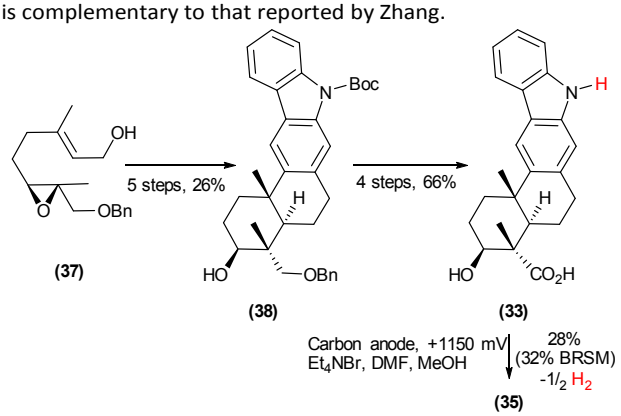

Scheme 7: Total synthesis of dixiamycin B (**35**) from chiral oxirane **37** by N-N dimerisation of xiamycin A (**33**)

The biosynthetic origins of the dixiamycins have been the subject of several recent studies,[78, 79, 82, 83] such that there is substantial evidence that xiamycin A is derived from the sesquiterpene-bound indole indosespene by the action of the *xia* gene cluster of *Streptomyces* species. The exact mechanism for the dimerisation of xiamycin A to dixiamycins has not been fully elucidated, however it has been proposed that dimerisation occurs by a XiaH-mediated radical homocoupling.[79] Preliminary antibacterial testing of **34** and **35** found greater activity against four indicator strains compared with that of related monomers, including **33**. MIC values between 4-16 μg.mL^{-1} were obtained for susceptible strains of *E. coli*, *S. aureus*, *B. subtilis*, and *B. thuringensis*. Though there are no current studies indicating useful pharmacological applications of the two atropdiastereomers, the remarkable stability of their N-N axes to acid, UV irradiation and heat could be utilised in the future.[81]

3.4 Streptorubin B: A recently synthesized antibiotic from red pigments in *Streptomyces*

The prodiginine family of molecules are produced in a wide array of bacteria and marine organisms, and exhibit a wide array of biological activities.[84] One such member of this family was extracted from the pigment of several *Streptomyces* species in 1975 by the Gerber group using chromatographic techniques, and initially assigned the structure **39** (Figure **12**) using mass spectral, UV-vis, and NMR analysis.[85] A revision of this structure to **40** (Figure **12**) came three years later by the same author,[86] though confusion surrounding the correct structure and atropisomeric potential of the natural product remained,[87, 88] until relatively recent studies put any ambiguities to rest and confirmed the correct general structure as **40**.[89, 90]

It was in a study by Challis *et al* in 2010 that NOESY correlations of the HCl salts of extracted streptorubin B allowed for assignment of the major naturally occurring product as being the *anti*-configuration with regards to the positioning of the C7' *n*-butyl group relative to rings A and B, with the *syn* configuration only present in minor amounts.[91] Mutasynthesis with deuterium labelled precursors allowed the group to determine the stereochemistry of the C7' in the naturally produced streptorubin B to be a ratio of 88:7:5 for (7'*S*, *anti*):(7'*S*, *syn*):(7'*R*, *anti*), respectively, confirmed by X-ray crystallography analysis. Importantly, Challis *et al* noted that reanalysis of the separated products following chiral HPLC did not immediately show interconversion of the *anti* (**40**) to the *syn* (**41**), however a mixture of the two was observed after being allowed to stand at RT for 7 days, indicating slowed rotation about the atropisomeric axes.

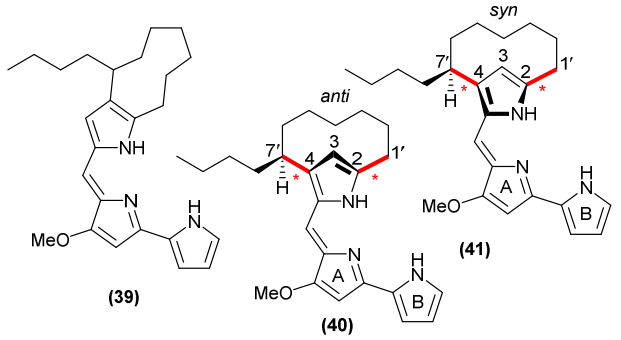

Figure 12: The initial incorrect structure (butylcycloheptylprodigiosin, BCHP) attributed to streptorubin B (**39**), and the confirmed absolute structures of major natural product (7'*S*, *anti*) streptorubin B (**40**) and the minor product (7'*S*, *syn*) streptorubin B (**41**), with the minor (7'*R*, *anti*) isomer not shown.

Parallel to this study, the first total synthesis of **40** by Thompson *et al* arrived at the same conclusion of absolute configuration.[92] This investigation first utilised an approach of ring closing metathesis to generate the streptorubin core; however this approach failed, presumably due to ring strain of the desired product. Thus, a new method was developed (Scheme **8**) using a Swern oxidation of intermediate **42** (generated from an enantioselective aldol/Wittig reaction of heptanedial) followed by enantioselective addition of a protected alkenyl to furnish **43**. When subjected to KHMDS, this intermediate underwent an anionic oxy-Cope oxidative rearrangement to form **44**, which was subjected to catalytic hydrogenation, Dess-Martin oxidation, and a Paal-Knorr pyrrole generation to form **45**, which underwent a condensation with aldehyde **46** to form **41**, which on standing converted to the presumably more stable **40**, indicating that the natural product is the more thermally stable configuration. Using further NMR analysis, it was found that the ratio of equilibrated *anti*:*syn* streptorubin B at room temperature was approximately 10:1, with an interconversion barrier of 20.5 kcal/mol. X-ray crystallography of HCl salts for both synthetic and natural products confirmed the absolute configuration of the primary product as **40** using anomalous dispersion calculations.[92]

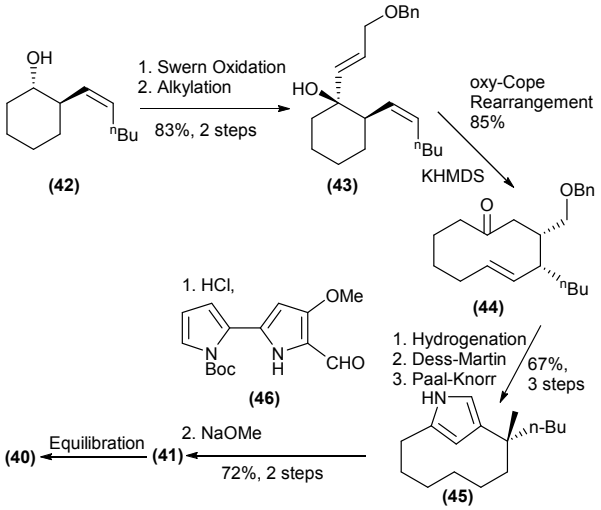

Scheme 8: The first total-synthesis of streptorubin B, the main product being the *syn* isomer (**41**), which equilibrated over time to give the more stable *anti* configuration (**40**).

The biosynthetic pathway of streptorubin B has been found to share common precursors with other prodiginines of similar structure.[91] Using extensive biogenetic studies, Challis *et al* determined that the enzyme RedH catalyses the condensation of 2-undecypyrrole (Scheme **9**, Compound **47**) with 4-methoxy-2,2'-bipyrrole-5-carboxaldehyde (**48**) to form an acyclic precursor undecylprodigiosin (**49**), which subsequently undergoes oxidative cyclisation catalysed by RedG to form streptorubin B.[93] The mechanism of this oxidation had recently been determined to proceed through abstraction of the *pro-R* proton from the C7' position by an Fe(III)OOH complex in the active site of the protein, with inversion of this C7'.[94]

The prodiginine family, including streptorubin B, have proven to have relatively potent antimalarial activity,[85, 95] however have too narrow a therapeutic window for direct medicinal application. However, some prodiginines have recently proven to have apoptotic action against a variety of cancer cell lines, including hepatocellular carcinoma (for which there is currently no effective treatment); though the extent of healthy

cell DNA damage and cyctotoxicity have not been fully explored.[84, 96]

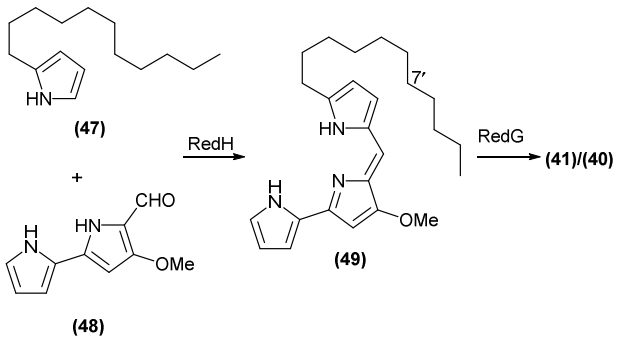

Scheme 9: The biosynthetic pathway of streptorubin B in *Streptomyces Coelicolor* A3(2).

3.5 Ustiloxins A-F: Recent total synthesis of potent atropisomeric antimitotic agents

Antimitotic agents are of considerable importance in the chemotherapeutic treatment of a variety of cancer types, as they collectively interfere with eukaryotic cell mitosis. These prevent cell mitosis through a variety of mechanisms, depending on the specific drug, the most prevalent of which is through inhibition of tubulin polymerization during the formation of microtubules.[97] Alongside well-known vinca alkaloids, some naturally-occurring peptidic molecules elicit such inhibition, including the atropisomeric ustiloxin family of molecules, which target the α,β-tubulin dimer. These cyclodepsipeptides were discovered in 1992, within deposits formed by a rice pathogen *Ustilaginoidea virens*.[98] Similar in structure to the previously identified phomopsin family, these molecules were found to have inhibitory activity on brain tubulin,[99, 100] though had much lower cytotoxic potential than many other antimitotic agents.[101]

The recent total synthesis of the ustiloxins has allowed for SAR studies to be conducted on a variety of analogues, which has served the dual purpose of revealing key interactions of the relatively ambiguous mode of inhibition, and allowing the production of more effective antimitotic drugs.[101, 102] Ustiloxin D (Figure **13**, Compound **50**) was used as an initial synthetic target, given its simple structure and that it demonstrated the highest biological activity of all members of the ustiloxin family. Structurally, it is a simple cyclodepsipeptide comprised of four amino acid residues (namely glycine, valine, and derivatives of isoleucine and tyrosine), however the atropisomeric nature of the alkyl-aryl ether bond posed a number of synthetic challenges, including how best to selectively induce axial chirality without impacting pre-existing point-chiral elements, while maintaining functional group tolerance.[101] The atropisomerism of this molecule was assigned using ^{1}H-^{1}H NOESY, and found to only be naturally present in the *syn* form.

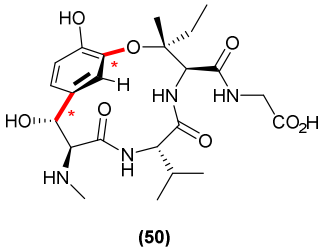

Figure 13: The absolute structure of ustiloxin D (**50**), as determined by NOE spectroscopy, with likely key bonds regarding atropisomeric nature indicated with an asterisk (*).

The first successful approach in the generation of ustiloxin D was a linear total synthesis consisting of 31 steps, with an 82% yield on average for each step.[103] This process, summarised below (Scheme **10**), first required the formation of an amino alcohol (**51**) from D-serine in 8 steps. The ether (**53**) was then generated by nucleophilic aromatic substitution of aryl fluoride (**52**) with **51**. Atropselectivity about the ether is kinetically driven during the macrolactamization of **54**, ensuring that peptide coupling can only occur in the *syn* configuration. With the basic scaffold completed, the resulting macrocycle (**55**) was subjected to several deprotection and functionalization reactions to generate ustiloxin D (**50**) in a 4.3% overall yield from **51**.

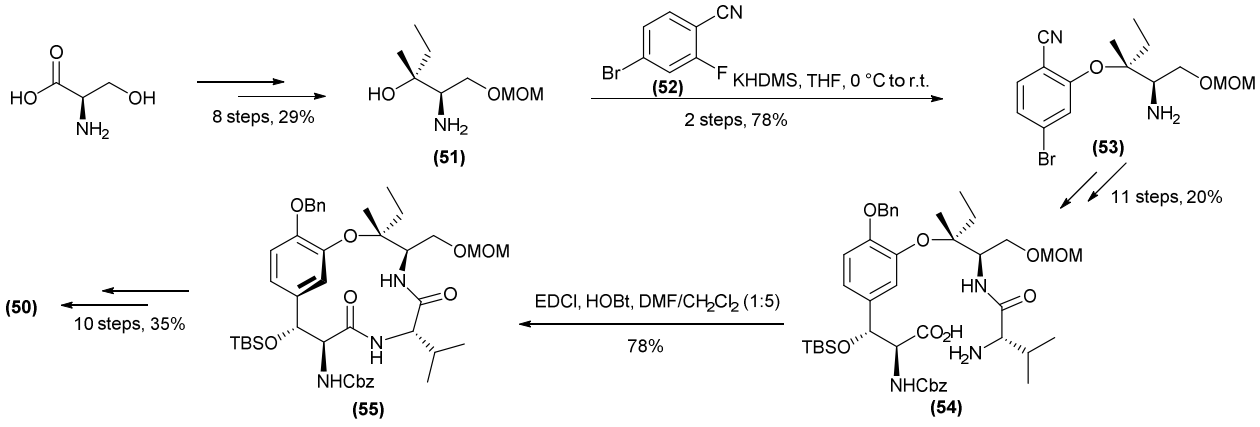

Scheme 10: Linear synthesis of Ustiloxin D (**50**) from protected amino alcohol **51**.

NPR

Review

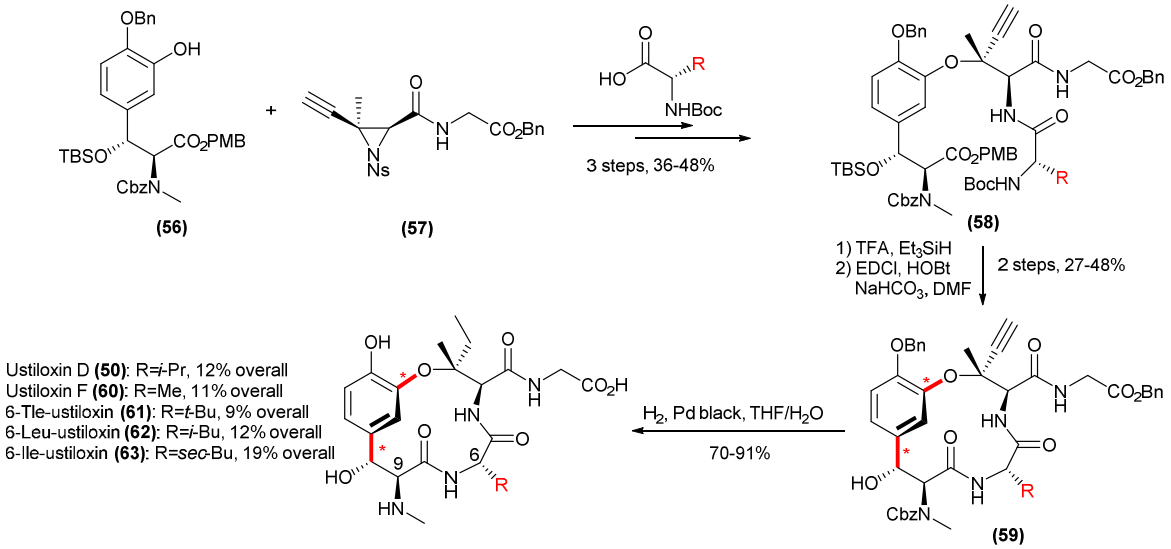

Scheme 11: Convergent synthetic approach towards the generation of ustiloxin D (**50**), ustiloxin F (**60**), and a variety of derivatives (**61-63**).

The need for further SAR studies required the development of a more tolerant synthesis which could accommodate variations in functionalization was needed. As such, an optimized second generation, convergent synthesis was devised by Joullié *et al*,[101] and is depicted in Scheme **11**. This modular strategy relies firstly on the phenol-mediated ring-opening of ethynyl aziridine **57**, and subsequent deprotection and peptide coupling with a Boc-protected amino acid affords intermediate scaffold **58**. Further deprotection of the Boc and PMB groups allows access to the free carboxylate and terminal amine, and EDCI-HOBt-mediated peptide coupling affords the macrocycle **59**, of which the axial chirality is ensured by the kinetic stability of the *cis* configuration during intramolecular coupling. Finally, catalytic hydrogenation concurrently leads to both Bn and Cbz deprotection, and the hydrogenation of the pendant alkyne to generate the desired ustiloxin analogues in higher yields permitted by the aforementioned linear synthesis. Furthermore, this protocol allowed for simpler modulation of substituents, allowing for the generation of ustiloxin D, ustiloxin F, and a variety of derivatives to ascertain important structural characteristics for testing of inhibition of tubulin polymerization.

Biological testing revealed that modifications to the C6 position were generally well tolerated, as shown in Table **1**, and also that a compacted but highly branched aliphatic unit at this position is most beneficial. Alterations to the phenol hydroxyl group, and inversion of the natural (9*S*)-methylamino group to a (9*R*)-methylamino stereochemistry however resulted in total loss of inhibition, implying these positions are critical for tubulin binding. Though the atropisomeric contribution to activity has not been explored, it is crucial to recognise the importance of the development of synthetic techniques allowing for the production of the atropisomeric ustiloxin family. This natural product has given important insight into the mode of action of α,β-tubulin dimer inhibition, vital for oncological studies, and armed with this information, more effective anticancer drugs devised.

Table 1: Inhibition of tubulin polymerization by a variety of ustiloxin derivatives with C6 modulation.

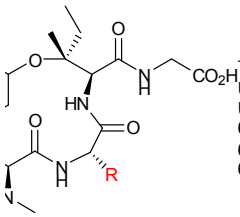

Compounds	IC50 (mM)
Ustiloxin D: R=i-Pr	1.5 ± 0.4
Ustiloxin F: R=Me	8.2 ± 1.0
6-Tle-ustiloxin: R=t-Bu	1.2 ± 0.02
6-Leu-ustiloxin: R=i-Bu	8.2 ± 0.04
6-Ile-ustiloxin: R=sec-Bu	4.8 ± 0.04

3.6 Haouamine A: Natural atropisomeric alkaloid with a complex structure and synthesis

The sheer complexity of a variety of marine natural products has provided challenging synthetic targets in the field of medicinal chemistry, and has historically served as impetus for the development of selective, efficient and scalable synthetic methodologies to allow such complex architectures to be targeted. The discovery of Haouamine A (Figure **14**, Compound **64**) from a species of ascidian (sea squirt)[104] provided a unique molecular structure following extensive NMR analysis and X-ray crystallography. This structure contained a *p*-cyclophane moiety, a biaryl axis with a relatively unique, highly strained

'bent' benzene ring,[105] and a spiro fused-ring system. The originally isolated molecule was observed to contain two rapidly-interconverting isomers; the cause for this was thought to be the result of either a slowed pyramidal inversion of the sp^3 nitrogen, or the presence of an atropisomer (Figure **14**, compound **19**).[104] Computational modelling studies indicated a pyrimidal nitrogen inversion to be the more likely cause of this interconversion, however to confirm the configurational stability of the biaryl axis, an atropselective total synthesis had to be devised, which was eventually realised by Baran *et al*. [106]

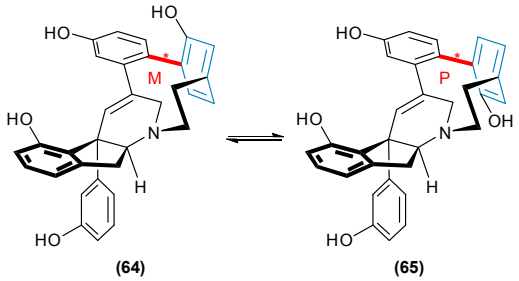

Figure 14: The structure of Haouamine A (**64**) and its atropisomer (**65**), with the highly uncommon distorted benzene ring shown in blue.

Scheme **12** demonstrates the first- and second-generation syntheses of Hauoamine A from the divergent intermediate **66**, quickly assembled from a commercially-available indanone by a cascade annulation. Stille coupling of the Boc-protected polycycle (Route **A**), followed by deprotection and subsequent *N*-alkynylation afforded the primary foundation of the cyclophane system, and subsequent demethylation, peracetylation and a microwave-induced [4+2]-cycloaddition-decarboxylation afforded a racemic mixture of *(M)*- and *(P)*-Hauoamine A.[107] Attempts at modifying the cyclophane-forming cycloaddition step for enhanced atropselectivity were unsuccessful, hence a second-generation synthesis (Route **B**) was devised, which instead utilised a point-to-axial chirality transfer from a stereogenic tether. Suzuki coupling of the boronic acid derivative of **66** (prepared from the bromide by sequential lithiation, borylation [$B(OMe)_3$], and hydrolysis) afforded a stereogenic tosylate intermediate, which upon cyclisation afforded a separable mixture of cyclophanes in a ratio of 1.45(*M*):1(*P*). The *(M)*-isomer was selected, and oxidation of the tetrahedral centre with LiHMDS and *N*-*tert*-butylbenzenesulfinimidoyl chloride and subsequent global demethylation afforded enantiopure *(M)*-haouamine A in 17% yield (based on recovered starting material) from **66**.[106] This approach was found to be amenable to scale-up, and use of the *(P)*-cyclophane afforded *atrop*-haouamine A (**65**) in comparable yields (15% from **66**). Analysis of the CD spectra of *(P)*-**65** revealed mirrored characteristics to those of both synthetically-derived, and a sample of naturally-derived *(M)*-**64**, confirming the absolute configuration of the synthesised material, as well as the *(M)*-configuration of the natural product. Furthermore, the synthesis of both stable atropisomers by this methodology confirms the aforementioned rapid structural interconversion to be the result of a slowed pyramidal nitrogen inversion, and not the result of rapidly interconverting atropisomers or rotamers.

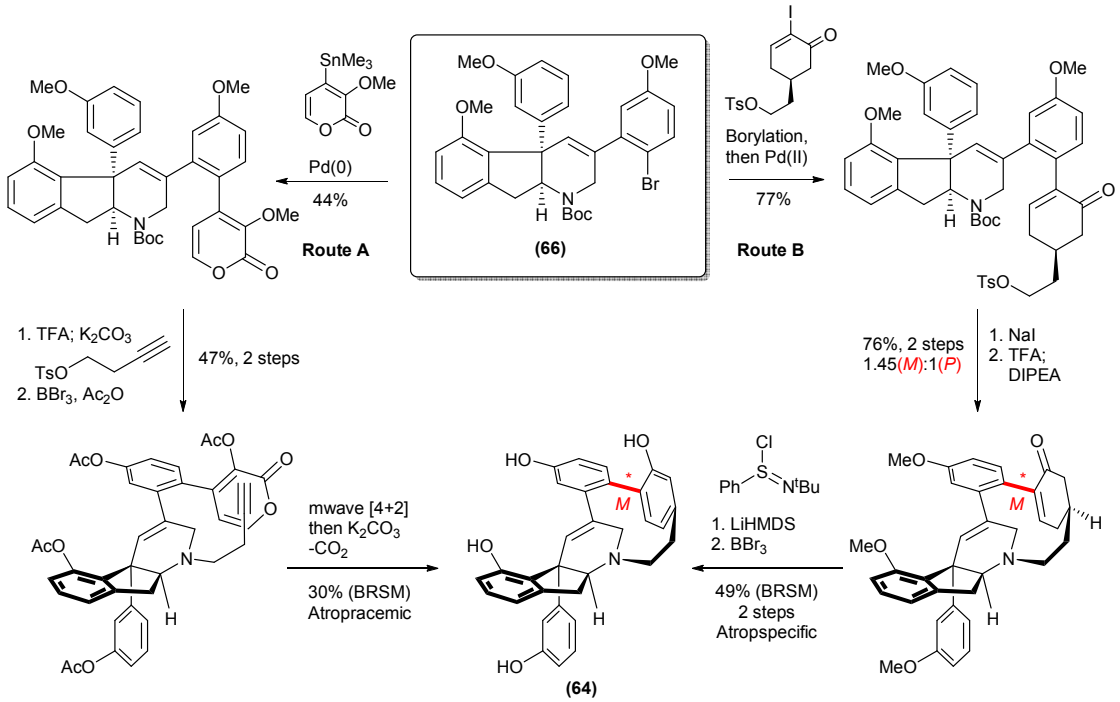

Scheme 12: The first- (**Route A**) and second-generation (**Route B**) syntheses of Haouamine A by the Baran group.

NPR

Review

Biosynthetic studies of the haouamines had indicated a Chichibabin pyridine synthesis to be the most apparent source for the central piperidine ring, however more recent studies have suggested a number of inconsistencies with such a hypothesis.[108] The biogenesis of the haouamines is therefore yet to be fully elucidated.

Both **64** and **65** displayed selective cytotoxic activity for HT-29 human colon carcinoma, and potent inhibition of PC3 human prostate cancer cells. This activity was found to be innately linked to the strained cyclophane moiety of Haouamine A, and moderate activities towards PC3 were identified for both atropisomers, with **64** exhibiting an IC_{50} value of 29 ± 2 μM, and **65** showing similarly potency (IC_{50} = 32 ± 3 μM).[106]

3.7 Bisnicalaterines: Unique atropisomeric antimalarials from traditional medicine

The discovery of new biologically-active molecules is often driven by the desire to characterise the active constituents of traditional medicinal plants. Traditionally used in the treatment of skin irritation and bacterial yaws, the leaves, bark and latex of *Hunteria Zeylanica* have been the subject of a number of investigations by multiple groups, resulting in the discovery of more than thirty indole and tetrahydrocarbazole alkaloids.[109-111] A recent investigation of *Hunteria Zeylanica* by Morita *et al.* led to the isolation and identification of a new class of biindole alkaloids, dubbed bisnicalaterines A-D (Figure **15**).[112-114]

Globally, the bisnicalaterines are defined by the presence of a biindole skeleton, with **67** being comprised of a pair of N,C-linked vobasine monomers, and **68**-**70** comprised of eburnane and coryanthe-type monomers, linked by an aryl-alkyl or aryl-alkenyl bond. In all cases, the bridge between the two substructures infers an atropisomeric effect; most notably, bisnicalaterines B and C differ only in the stereochemistry about the axis, being the *(P)* and *(M)* isomers, respectively. The atropisomeric nature of bisnicalaterines A-C (**67-69**) in particular is unusual, as rotation is restricted about a point-chiral sp^2-sp^3 bond, resulting in both point and axial chirality at a single stereogenic atom.

The divobasine structure of bisnicalaterine A was elucidated by exhaustive 2D NMR spectral analysis.[112] Analysis of the CD spectra revealed a strong positive first Cotton effect, and a negative second Cotton effect, which Morita *et al* interpreted as inferring a right-handed helix, and as such, the assigned *(M)*-configuration. This assignment was supported by NOESY experiments, which showed through-space correlation of H3-H3', and between H12' and the distal methylene proton at H14. The corynanthe-eburnane structures of Bisnicalaterines B (**68**) and C (**69**) were similarly identified by extensive 2D NMR

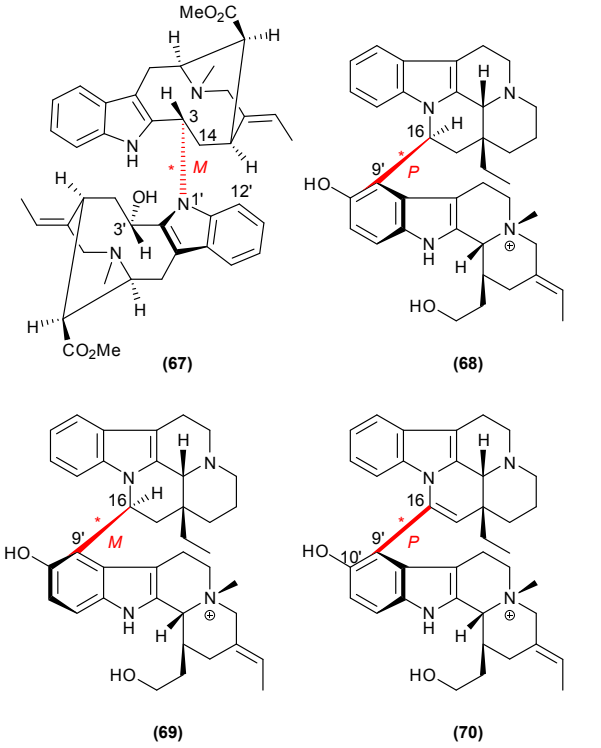

Figure 15: Determined structures of bisnicalaterines A (**67**), B (**68**), C (**69**), and D (**70**), and the stereochemistry about each axis.

experiments, which revealed a number of common HMBC and COSY correlations.[113] IR spectroscopic analysis uncovered the presence of a hydroxyl group, identified as being located as C10', *ortho* to the C9' axis. The acquisition of compatible HRESI-MS spectra, and near-identical IR spectra suggested the pair to be stereoisomers of one another. The nature of this isomerism was discovered by the acquisition of CD spectra for both species, which confirmed the pair to be atropisomers of each other, and comparison of the experimental CD spectrum with the calculated TD-DFT CD spectra allowed for the absolute assignment of the axes as *(P)* and *(M)* for **68** and **69**, respectively, which was supported by a number of NOESY-NMR correlations. Basic computational modelling of the global energy minimum conformation of each species suggested that the *(P)* isomer **68** exists in a twisted configuration, while its atropenantiomer adopts an extended, pseudo-linear geometry.

Similarly to **68** and **69**, bisnicalaterine D (**70**) was found to be composed of a coryanthe-eburnane scaffold by 2D NMR analysis, however the atropisomeric axis C16 was found to be oxidised, such that the point-chiral stereocentre had been

eliminated. Analysis of the NOESY spectrum inferred a twisted conformation about the axis, and while no theoretical TD-DFT CD calculations were undertaken, comparison of the experimental CD spectrum with that of bisnicalaterine B, and identification of a number of similarities allowed the axis to be assigned as being the *(P)* isomer.

Biological testing of these compounds revealed significant activities against a series of agonists. Bisnicalaterine A exhibits moderate activity against five human cancer cell lines, with IC_{50} values against HL-60, RPMI-8226, NCI-H226, HCT-116, and MCF-7 of 16.2, 31.3, 28.1, 21.9, and 38.0 $\mu g.mL^{-1}$, respectively.[112] Bisnicalaterines B (**68**) and C (**69**) were found to have vasorelaxant activity, of which **68** showed a maximal relaxation of 86.6 ± 4.9% in endothelium-intact rodent aortic rings, which was partially attributed to the opening of K^+ channels,[113] however the complete mechanism for this activity has currently not been fully elucidated. Most interestingly, bisnicalaterines **67**-**69** each showed high potency in antiplasmodial assays against *P. falciparum*, with **67**, **68** and **69** demonstrating IC_{50} and SI values of 4.36 µM (3.7), 1.13 µM (>47) and 0.05 µM (>1000), respectively. The outstanding potency and selectivity of **69**, compared with its atropisomer **68** illustrates a perfect example of the significance of atropisomerism in drug design and modern organic synthesis, as mediation of the axial helicity allows for enhanced activity and selectivity – in this instance allowing for the potency of this drug to be improved by two orders of magnitude.

While there have been no attempted syntheses of this class of compounds to date, their potency and selectivity warrants closer investigation, dictating the need for a modular synthetic route which may tolerate the variety of functional groups necessary for further SAR studies.

3.8 Tedarene B: The smallest central, planar, and axially-chiral molecule

The development of new methods for the isolation and characterisation of cyclophane natural products has led to a growing appreciation of planar chirality – and as such, atropisomerism – in the field of natural products chemistry. Combined instances of central and axial chirality are known to exist, as in the previously-mentioned example of the bisnicalaterines, however the recent discovery of the diarylheptanoid Tedarene B (Figure **16**, compound **71**) from extracts of the widespread marine sponge *Tedania ignus* marked a rare example of a natural product containing axial, planar and point-chiral elements.[115] Though Tedarene B has been briefly mentioned in recent reviews,[116-118] its nature as a unique atropisomeric architecture, combined with the brevity of previous reviews warrants its mention herein.

The diarylheptanoid scaffold is common to a number of bioactive natural products which have been isolated from terrestrial plant species. Sequential extraction of *T. ignus* with chloroform and methanol afforded a crude extract, which upon purification by reverse-phase chromatography and HPLC separation yielded Tedarene B, as well as an ether-bridged diarylheptanoid dubbed Tedarene A (**72**). While MD

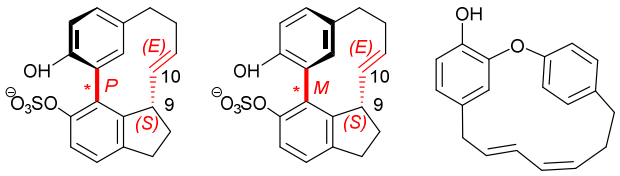

Figure 16: The structure of Tedarene B (**71**) in the native *(P)* configuration, and its *(M)* atropenantiomer (*atrop*-**71**), hindered by both its 10-(*E*) and 9-(*S*) stereochemistry. Tedarene A (**72**) was also isolated, though found to be anatropisomeric due to an insufficient rotational energy barrier about the diene.

simulations revealed a hindered rotation about the diene, the rotational energy barrier for **72** was calculated to be 14.0 ± 0.4 $kcal.mol^{-1}$ - falling short of the aforementioned requirement of a 23.3 $kcal.mol^{-1}$ barrier to be defined as atropisomeric - as such while rotation about the diene is slowed, and may be sufficiently hindered that both conformers may be visible on an NMR time-scale, **72** likely exists instead as a pair of rotomers, and not as distinctly separable atropisomers

The broad structure of **71** was elucidated by a number of 2D NMR experiments and HR-ESI-MS, of which NMR analysis revealed an equilibrium mixture of a pair of conformers in a 4:1 ratio, attributed to the slow rotation of the alkene moiety. Comparison of obtained CD spectra with a calculated CD spectrum (TD-DFT) allowed the assignment of the biaryl axis as the *(P)* isomer. MD simulations (1500 K, 100 ns) supported this assignment, demonstrating the *(P)* isomer to be stable, while the *(M)* isomer was found to quickly invert to the *(P)* after 20-40 ns, indicating the *(P)* isomer to be thermodynamically favourable.

The biosynthetic origins of diarylheptane scaffolds as the product of functionalisation of phenylpropanoids with malonyl COA are well-known.[119, 120] Diarylheptanoids as a class of molecules have previously been identified as possessing a variety of bioactive effects,[121, 122] and though it has been noted that cyclic diarylheptanoids have been shown to exhibit inhibitory activity against LPS-induced NO production,[123, 124] preliminary testing indicated Tedarene B to be inactive. Due to the small sample size however, little further testing has been undertaken, and as such its efficacy as a potential therapeutic species has not yet been fully elucidated. Furthermore, despite its relatively small and accessible carbocyclic skeleton, no total synthesis has been devised as yet to allow for application toward biological testing or derivative generation.

5. Conclusions

Though the utility of atropisomeric natural products has been well established in recent years, characterization of these compounds is subject to inconsistencies in both identification and classification. While it is common to measure the optical activity of newly-discovered molecules, the source from which variations in rotation arise is not always explored. As such, rotational characteristics are often solely attributed to chiral centres, dismissing the effect of potentially atropisomeric systems. Substituted biaryl systems are relatively common

throughout nature, and to avoid ambiguity, recognition of the contribution of atropisomers to optical activity should be more widely investigated. Through wider recognition of these peculiarities, the study of such molecules may become fully appreciable and accessible.

This being the case, it is evident that natural atropisomerism is a valuable resource from which potential drug leads may be obtained, and the specificity evident in atropisomeric molecules could prove vital in the development of targeted therapies for almost all areas of disease. By improving current techniques to control the isomerism, a new realm of synthetic molecules may be explored, and more complex moieties may become available.

Abbreviations

CAMKIII – Calmodulin-Dependent Protein Kinase III
CBD – Cannibidiol
CIP – Cahn-Ingold-Prelog Priority Rules
DAD – Photodiode Array Detection
d.r. – Diastereomeric Ratio
ECD – Electronic Circular Dichroism
e.e – Enantiomeric Excess
HPLC – High-Performance Liquid Chromatography
HR-ESI/MS – High-Resolution Electrospray Ionization Mass Spectrometry
HR-FAB/MS – High-Resolution Fast Atom Bombardment Mass Spectrometry
MIC – Minimum Inhibitory Concentration
MRSA – Methicillin-resistant Staphylococcus aureus
NMR – Nuclear Magnetic Resonance
PC3 –Prostate Cancer cell line 3
PKA – Protein Kinase A
PKC – Protein Kinase C
rac - Racemic
TD-DFT – Time-Dependent Density Function Theory
UV – Ultraviolet
VA – Vibrational Absorption
VCD – Vibrational Circular Dichroism

Conflict of Interest

The author confirms that this article content has no conflict of interest

Acknowledgements

We thank Dr. Danielle Skropeta for her advice with this review.

Notes and references

1. M. Ōki, in *Topics in Stereochemistry*, John Wiley & Sons, Inc., 1983, pp. 1-81.
2. G. Bringmann, T. Gulder, T. A. M. Gulder and M. Breuning, *Chem. Rev.*, 2011, **111**, 563-639.
3. G. Bringmann, A. J. P. Mortimer, P. A. Keller, M. J. Gresser, J. Garner and M. Breuning, *Angew. Chem. Int. Ed.*, 2005, **44**, 5384-5427.
4. M. H. McCormick, J. M. McGuire, G. E. Pittenger, R. C. Pittenger and W. M. Stark, *Antibiot. Annu.*, 1955, **3**, 606-611.
5. D. H. Williams and B. Bardsley, *Angew. Chem. Int. Ed.*, 1999, **38**, 1172-1193.
6. M. Farooq, W. L. Tarar, F. Amin Dr and K. T. Mahmood, *J. Pharm. Sci. Res.*, 2011, **3**, 1599-1603.
7. K. Sprogøe, D. Stærk, H. L. Ziegler, T. H. Jensen, S. B. Holm-Møller and J. W. Jaroszewski, *J. Nat. Prod.*, 2008, **71**, 516-519.
8. L. Zhang, H. Jiang, X. Cao, H. Zhao, F. Wang, Y. Cui and B. Jiang, *Eur. J. Med. Chem.*, 2009, **44**, 3961-3972.
9. G. Bringmann and F. Pokorny, in *Alkaloids*, Academic Press, 1995, vol. 46, pp. 127-271.
10. G. Bringmann, *Bull. Soc. Chim. Belg.*, 1996, **105**, 601-613.
11. G. Bringmann, A. Irmer, D. Feineis, T. A. M. Gulder and H. P. Fiedler, *Phytochemistry*, 2009, **70**, 1776-1786.
12. G. Bringmann, B. K. Lombe, C. Steinert, K. N. Ioset, R. Brun, F. Turini, G. Heubl and V. Mudogo, *Org. Lett.*, 2013, **15**, 2590-2593.
13. K. Ramig, *Tetrahedron*, 2013, **69**, 10783-10795.
14. V. P. Nicu, A. Mándi, T. Kurtán and P. L. Polavarapu, *Chirality*, 2014, **26**, 525-531.
15. G. Bringmann, T. Bruhn, K. Maksimenka and Y. Hemberger, *Eur. J. Org. Chem.*, 2009, DOI: 10.1002/ejoc.200801121, 2717-2727.
16. P. J. Stephens, F. J. Devlin, C. F. Chabalowski and M. J. Frisch, *J. Phys. Chem.*, 1994, **98**, 11623-11627.
17. A. L. Albright and J. M. White, *Method. Mol. Biol.*, 2013, **1055**, 149-162.
18. T. Kajiura, T. Furumai, Y. Igarashi, H. Hori, K. Higashi, T. Ishiyama, M. Uramoto, Y. Uehara and T. Oki, *J. Antibiot.*, 1998, **51**, 394-401.
19. H. Hori, Y. Igarashi, T. Kajiura, T. Furumai, K. Higashi, T. Ishiyama, M. Uramoto, Y. Uehara and T. Oki, *J. Antibiot.*, 1998, **51**, 402-417.
20. I. M. Romaine, J. E. Hempel, G. Shanmugam, H. Hori, Y. Igarashi, P. L. Polavarapu and G. A. Sulikowski, *Org. Lett.*, 2011, **13**, 4538-4541.
21. K. Tatsuta, T. Fukuda, T. Ishimori, R. Yachi, S. Yoshida, H. Hashimoto and S. Hosokawa, *Tetrahedron Lett.*, 2012, **53**, 422-425.
22. K. Tatsuta and S. Hosokawa, *Chem. Rec.*, 2014, **14**, 28-40.
23. B. B. Liau, B. C. Milgram and M. D. Shair, *J. Am. Chem. Soc.*, 2012, **134**, 16765-16772.
24. T. Kajiura, T. Furumai, Y. Igarashi, H. Hori, K. Higashi, T. Ishiyama, M. Uramoto, Y. Uehara and T. Oki, *J. Antibiot.*, 2002, **55**, 53-60.
25. H. Hori, T. Kajiura, Y. Igarashi, T. Furumai, K. Higashi, T. Ishiyama, M. Uramoto, Y. Uehara and T. Oki, *J. Antibiot.*, 2002, **55**, 46-52.
26. I. M. Romaine and G. A. Sulikowski, *Tetrahedron Lett.*, 2015, **56**, 3617-3619.
27. S. I. Cho, H. Fukazawa, Y. Honma, T. Kajiura, H. Hori, Y. Igarashi, T. Furumai, T. Oki and Y. Uehara, *J. Antibiot.*, 2002, **55**, 270-278.
28. A. H. Aly, A. Debbab and P. Proksch, *Appl. Microbiol. Biotechnol.*, 2011, **90**, 1829-1845.

29. R. Bara, I. Zerfass, A. H. Aly, H. Goldbach-Gecke, V. Raghavan, P. Sass, A. Mandi, V. Wray, P. L. Polavarapu, A. Pretsch, W. Lin, T. Kurtan, A. Debbab, H. Brotz-Oesterhelt and P. Proksch, *J. Med. Chem.*, 2013, **56**, 3257-3272.
30. J. Atherton, B. W. Bycroft, J. C. Roberts, P. Roffey and M. E. Wilcox, *J. Chem. Soc. C*, 1968, 2560-2564.
31. P. L. Polavarapu, N. Jeirath, T. Kurtán, G. Pescitelli and K. Krohn, *Chirality*, 2009, **21**, E202-E207.
32. A. R. B. Ola, A. Debbab, T. Kurtán, H. Brötz-Oesterhelt, A. H. Aly and P. Proksch, *Tetrahedron Lett.*, 2014, **55**, 3133-3136.
33. A. Urban, S. Eckermann, B. Fast, S. Metzger, M. Gehling, K. Ziegelbauer, H. Rübsamen-Waigmann and C. Freiberg, *Appl. Environ. Microbiol.*, 2007, **73**, 6436-6443.
34. N. Au, E. Kuester-Schoeck, V. Mandava, L. E. Bothwell, S. P. Canny, K. Chachu, S. A. Colavito, S. N. Fuller, E. S. Groban, L. A. Hensley, T. C. O'Brien, A. Shah, J. T. Tierney, L. L. Tomm, T. M. O'Gara, A. I. Goranov, A. D. Grossman and C. M. Lovett, *J. Bacteriol.*, 2005, **187**, 7655-7666.
35. D. J. Haydon, N. R. Stokes, R. Ure, G. Galbraith, J. M. Bennett, D. R. Brown, P. J. Baker, V. V. Barynin, D. W. Rice, S. E. Sedelnikova, J. R. Heal, J. M. Sheridan, S. T. Aiwale, P. K. Chauhan, A. Srivastava, A. Taneja, I. Collins, J. Errington and L. G. Czaplewski, *Science*, 2008, **321**, 1673-1675.
36. J. Wang, A. Galgoci, S. Kodali, K. B. Herath, H. Jayasuriya, K. Dorso, F. Vicente, A. González, D. Cully, D. Bramhill and S. Singh, *J. Biol. Chem.*, 2003, **278**, 44424-44428.
37. D. Weisleder and E. B. Lillehoj, *Tetrahedron Lett.*, 1971, **12**, 4705-4706.
38. K. Suzuki, K. Nozawa, S. Nakajima and K. I. Kawai, *Chem. Pharm. Bull.*, 1990, **38**, 3180-3181.
39. Y. S. Park, C. I. Grove, M. González-López, S. Urgaonkar, J. C. Fettinger and J. T. Shaw, *Angew. Chem. Int. Ed.*, 2011, **50**, 3730-3733.
40. C. I. Grove, J. C. Fettinger and J. T. Shaw, *Synthesis*, 2012, **44**, 362-371.
41. D. T. Wong and R. L. Hamill, *Biochem. Biophys. Res. Commun.*, 1976, **71**, 332-338.
42. M. H. Foss, Y. J. Eun, C. I. Grove, D. A. Pauw, N. A. Sorto, J. W. Rensvold, D. J. Pagliarini, J. T. Shaw and D. B. Weibel, *MedChemComm*, 2013, **4**, 112-119.
43. J. Liu, F. Li, E. La Kim, J. Hong and J. H. Jung, *Nat. Prod. Sci.*, 2013, **19**, 61-65.
44. S. Kundu, T. H. Kim, J. H. Yoon, H. S. Shin, J. Lee, J. H. Jung and H. S. Kim, *Int. J. Oncol.*, 2014, **45**, 2331-2340.
45. M. Stewart, R. J. Capon, J. M. White, E. Lacey, S. Tennant, J. H. Gill and M. P. Shaddock, *J. Nat. Prod.*, 2004, **67**, 728-730.
46. T. Qin, S. L. Skraba-Joiner, Z. G. Khalil, R. P. Johnson, R. J. Capon and J. A. Porco, *Nature Chemistry*, 2015, **7**, 234-240.
47. B. Bister, D. Bischoff, M. Ströbele, J. Riedlinger, A. Reicke, F. Wolter, A. T. Bull, H. Zähner, H. P. Fiedler and R. D. Süssmuth, *Angew. Chem. Int. Ed.*, 2004, **43**, 2574-2576.
48. A. Zask, J. Murphy and G. A. Ellestad, *Chirality*, 2013, **25**, 265-274.
49. V. Savic, in *Stud. Nat. Prod. Chem.*, 2013, vol. 40, pp. 133-172.
50. C. W. Zapf, B. A. Harrison, C. Drahl and E. J. Sorensen, *Angew. Chem. Int. Ed.*, 2005, **44**, 6533-6537.
51. K. C. Nicolaou and S. T. Harrison, *Angew. Chem. Int. Ed.*, 2006, **45**, 3256-3260.
52. S. Keller, H. S. Schadt, I. Ortel and R. D. Süssmuth, *Angew. Chem. Int. Ed.*, 2007, **46**, 8284-8286.
53. R. Peters and D. F. Fischer, *Angew. Chem. Int. Ed.*, 2006, **45**, 5736-5739.
54. F. Bihelovic, I. Karadzic, R. Matovic and R. N. Saicic, *Org. Biomol. Chem*, 2013, **11**, 5413-5424.
55. R. Matovic, F. Bihelovic, M. Gruden-Pavlovic and R. N. Saicic, *Org. Biomol. Chem*, 2014, **12**, 7682-7685.
56. F. Bihelovic and R. N. Saicic, *Angew. Chem. Int. Ed.*, 2012, **51**, 5687-5691.
57. E. M. Gottardi, J. M. Krawczyk, H. Von Suchodoletz, S. Schadt, A. Mühlenweg, G. C. Uguru, S. Pelzer, H. P. Fiedler, M. J. Bibb, J. E. M. Stach and R. D. Süssmuth, *ChemBioChem*, 2011, **12**, 1401-1410.
58. J. Riedlinger, A. Reicke, H. Zähner, B. Krismer, A. T. Bull, L. A. Maldonado, A. C. Ward, M. Goodfellow, B. Bister, D. Bischoff, R. D. Süssmuth and H. P. Fiedler, *J. Antibiot.*, 2004, **57**, 271-279.
59. K. C. Nicolaou and S. T. Harrison, *J. Am. Chem. Soc.*, 2007, **129**, 429-440.
60. J. S. Freundlich, M. Lalgondar, J. R. Wei, S. Swanson, E. J. Sorensen, E. J. Rubin and J. C. Sacchettini, *Tuberculosis*, 2010, **90**, 298-300.
61. D. L. J. Clive and P. Cheng, *Tetrahedron*, 2013, **69**, 5067-5078.
62. C. C. Hughes, C. A. Kauffman, P. R. Jensen and W. Fenical, *J. Org. Chem.*, 2010, **75**, 3240-3250.
63. C. C. Hughes, A. Prieto-Davo, P. R. Jensen and W. Fenical, *Org. Lett.*, 2008, **10**, 629-631.
64. C. Cheng, Y. Liu, M. E. Balasis, T. P. Garner, J. Li, N. L. Simmons, N. Berndt, H. Song, L. Pan, Y. Qin, K. C. Nicolaou, E. Gavathiotis, S. M. Sebti and R. Li, *Marine Drugs*, 2014, **12**, 4311-4325.
65. C. Cheng, Y. Liu, M. E. Balasis, N. L. Simmons, J. Li, H. Song, L. Pan, Y. Qin, K. C. Nicolaou, S. M. Sebti and R. Li, *Marine Drugs*, 2014, **12**, 1335-1348.
66. C. Cheng, Y. Liu, H. Song, L. Pan, J. Li, Y. Qin and R. Li, *Marine Drugs*, 2013, **11**, 2927-2948.
67. C. Cheng, L. Pan, Y. Chen, H. Song, Y. Qin and R. Li, *J. Comb. Chem.*, 2010, **12**, 541-547.
68. A. A. Kanakis and V. Sarli, *Org. Lett.*, 2010, **12**, 4872-4875.
69. Y. Liu, N. M. Haste, W. Thienphrapa, J. Li, V. Nizet, M. Hensler and R. Li, *Marine Drugs*, 2014, **12**, 2458-2470.
70. K. C. Nicolaou, N. L. Simmons, J. S. Chen, N. M. Haste and V. Nizet, *Tetrahedron Lett.*, 2011, **52**, 2041-2043.
71. P. Cheng, D. L. J. Clive, S. Fernandopulle and Z. Chen, *Chem. Commun.*, 2013, **49**, 558-560.
72. K. Yamanaka, K. S. Ryan, T. A. M. Gulder, C. C. Hughes and B. S. Moore, *J. Am. Chem. Soc.*, 2012, **134**, 12434-12437.
73. N. M. Haste, C. C. Hughes, D. N. Tran, W. Fenical, P. R. Jensen, V. Nizet and M. E. Hensler, *Antimicrob. Agents Chemother.*, 2011, **55**, 3305-3312.
74. R. Li, C. Cheng, M. E. Balasis, Y. Liu, T. P. Garner, K. G. Daniel, J. Li, Y. Qin, E. Gavathiotis and S. M. Sebti, *Eur. J. Med. Chem*, 2014, **90**, 315-331.
75. K. Doi, R. Li, S. S. Sung, H. Wu, Y. Liu, W. Manieri, G. Krishnegowda, A. Awwad, A. Dewey, X. Liu, S. Amin, C. Cheng, Y. Qin, E. Schonbrunn, G. Daughdrill, T. P. Loughran Jr, S. Sebti and H. G. Wang, *J. Biol. Chem.*, 2012, **287**, 10224-10235.

76. Q. Zhang, A. Mándi, S. Li, Y. Chen, W. Zhang, X. Tian, H. Zhang, H. Li, W. Zhang, S. Zhang, J. Ju, T. Kurtán and C. Zhang, *Eur. J. Org. Chem.*, 2012, 5256-5262.
77. L. Ding, J. Münch, H. Goerls, A. Maier, H. H. Fiebig, W. H. Lin and C. Hertweck, *Bioorg. Med. Chem. Lett.*, 2010, **20**, 6685-6687.
78. Z. Xu, M. Baunach, L. Ding and C. Hertweck, *Angew. Chem. Int. Ed.*, 2012, **51**, 10293-10297.
79. M. Baunach, L. Ding, T. Bruhn, G. Bringmann and C. Hertweck, *Angew. Chem. Int. Ed.*, 2013, **52**, 9040-9043.
80. I. Alkorta and J. Elguero, *Comput. Theor. Chem.*, 2011, **964**, 25-31.
81. B. R. Rosen, E. W. Werner, A. G. O'Brien and P. S. Baran, *J. Am. Chem. Soc.*, 2014, **136**, 5571-5574.
82. H. Li, Q. Zhang, S. Li, Y. Zhu, G. Zhang, H. Zhang, X. Tian, S. Zhang, J. Ju and C. Zhang, *J. Am. Chem. Soc.*, 2012, **134**, 8996-9005.
83. Q. Zhang, H. Li, S. Li, Y. Zhu, G. Zhang, H. Zhang, W. Zhang, R. Shi and C. Zhang, *Org. Lett.*, 2012, **14**, 6142-6145.
84. A. Fürstner, *Angew. Chem. Int. Ed.*, 2003, **42**, 3582-3603.
85. N. N. Gerber, *J. Antibiot.*, 1975, **28**, 194-199.
86. N. N. Gerber, A. G. McInnes, D. G. Smith, J. A. Walter, J. L. C. Wright and L. C. Vining, *Can. J. Chem.*, 1978, **56**, 1155-1163.
87. S. W. Tsao, B. A. M. Rudd, X. G. He, C. J. Chang and H. G. Floss, *J. Antibiot.*, 1985, **38**, 128-131.
88. A. Fürstner, K. Radkowski and H. Peters, *Angew. Chem. Int. Ed.*, 2005, **44**, 2777-2781.
89. B. T. Jones, D. X. Hu, B. M. Savoie and R. J. Thomson, *J. Nat. Prod.*, 2013, **76**, 1937-1945.
90. S. Mo, P. K. Sydor, C. Corre, M. M. Alhamadsheh, A. E. Stanley, S. Haynes, L. Song, K. A. Reynolds and G. L. Challis, *Chem. Biol.*, 2008, **15**, 137-148.
91. S. W. Haynes, P. K. Sydor, C. Corre, L. Song and G. L. Challis, *J. Am. Chem. Soc.*, 2011, **133**, 1793-1798.
92. D. X. Hu, M. D. Clift, K. E. Lazarski and R. J. Thomson, *J. Am. Chem. Soc.*, 2011, **133**, 1799-1804.
93. A. M. Cerdeño, M. J. Bibb and G. L. Challis, *Chem. Biol.*, 2001, **8**, 817-829.
94. D. M. Withall, S. W. Haynes and G. L. Challis, *J. Am. Chem. Soc.*, 2015, DOI: 10.1021/jacs.5b03994.
95. K. Papireddy, M. Smilkstein, J. X. Kelly, Shweta, S. M. Salem, M. Alhamadsheh, S. W. Haynes, G. L. Challis and K. A. Reynolds, *J. Med. Chem.*, 2011, **54**, 5296-5306.
96. D. Yamamoto, Y. Kiyozuka, Y. Uemura, C. Yamamoto, H. Takemoto, H. Hirata, K. Tanaka, K. Hioki and A. Tsubura, *J. Cancer Res. Clin. Oncol.*, 2000, **126**, 191-197.
97. A. Nagle, W. Hur and N. S. Gray, *Curr. Drug Targets*, 2006, **7**, 305-326.
98. Y. Koiso, M. Natori, S. Iwasaki, S. Sato, R. Sonoda, Y. Fujita, H. Yaegashi and Z. Sato, *Tetrahedron Lett.*, 1992, **33**, 4157-4160.
99. S. Iwasaki, *Med. Res. Rev.*, 1993, **13**, 183-198.
100. R. F. Ludueña, M. C. Roach, V. Prasad, M. Banerjee, Y. Koiso, Y. Li and S. Iwasaki, *Biochem. Pharmacol.*, 1994, **47**, 1593-1599.
101. P. Li, C. D. Evans, Y. Wu, B. Cao, E. Hamel and M. M. Joullié, *J. Am. Chem. Soc.*, 2008, **130**, 2351-2364.
102. M. M. Joullié, S. Berritt and E. Hamel, *Tetrahedron Lett.*, 2011, **52**, 2136-2139.
103. B. Cao, H. Park and M. M. Joullié, *J. Am. Chem. Soc.*, 2002, **124**, 520-521.
104. L. Garrido, E. Zubía, M. J. Ortega and J. Salvá, *J. Org. Chem.*, 2003, **68**, 293-299.
105. T. Gulder and P. S. Baran, *Nat. Prod. Rep.*, 2012, **29**, 899-934.
106. N. Z. Burns, I. N. Krylova, R. N. Hannoush and P. S. Baran, *J. Am. Chem. Soc.*, 2009, **131**, 9172-9173.
107. P. S. Baran and N. Z. Burns, *J. Am. Chem. Soc.*, 2006, **128**, 3908-3909.
108. N. Z. Burns and P. S. Baran, *Angew. Chem. Int. Ed.*, 2008, **47**, 205-208.
109. L. S. R. Arambewela and F. Khuong-Huu, *Phytochem.*, 1981, **20**, 349-350.
110. C. Lavaud, G. Massiot, J. Vercauteren and L. Le Men-olivier, *Phytochem.*, 1982, **21**, 445-447.
111. Y.-J. Xu, C.-P. Tang, C.-Q. Ke and Y. Ye, *Chem. Nat. Compd.*, 2009, **45**, 834-836.
112. A. E. Nugroho, Y. Hirasawa, N. Kawahara, Y. Goda, K. Awang, A. H. Hadi and H. Morita, *J. Nat. Prod.*, 2009, **72**, 1502-1506.
113. Y. Hirasawa, M. Hara, A. E. Nugroho, M. Sugai, K. Zaima, N. Kawahara, Y. Goda, K. Awang, A. H. Hadi, M. Litaudon and H. Morita, *J. Org. Chem.*, 2010, **75**, 4218-4223.
114. A. E. Nugroho, M. Sugai, Y. Hirasawa, T. Hosoya, K. Awang, A. H. Hadi, W. Ekasari, A. Widyawaruyanti and H. Morita, *Bioorg. Med. Chem. Lett.*, 2011, **21**, 3417-3419.
115. V. Constantino, E. Fattorusso, A. Mangoni, C. Perinu, R. Teta, E. Panza and A. Ianaro, *J. Org. Chem.*, 2012, **77**, 6377-6383.
116. R. A. Hill and A. Sutherland, *Nat. Prod. Rep.*, 2012, **29**, 829-833.
117. R. A. Hill, *Annu. Rep. Prog. Chem., Sect. B: Org. Chem.*, 2013, **109**, 146-166.
118. J. W. Blunt, B. R. Copp, R. A. Keyzers, M. H. G. Munro and M. R. Prinsep, *Nat. Prod. Rep.*, 2014, **31**, 160-258.
119. S. Kawai, K. Nakata, M. Ohashi and T. Nishida, *J. Wood. Sci.*, 2008, **54**.
120. J. R. Jones, M. D. Lebar, U. K. Jinwal, J. F. Abisambra, J. Koren, L. Blair, J. C. O'Leary, Z. Davey, J. Trotter, A. G. Johnson, E. Weeber, C. B. Eckman, B. J. Baker and C. A. Dickey, *J. Nat. Prod.*, 2011, **74**, 38-44.
121. M. Takahashi, H. Fuchino, S. Sekita and M. Satake, *Phytother. Res.*, 2004, **18**, 573-578.
122. H. Lv and G. She, *Rec. Nat. Prod.*, 2012, **6**, 321-333.
123. J. Tao, T. Morikawa, I. Toguchida, S. Ando, H. Matsuda and M. Yoshikawa, *Bioorg. Med. Chem.*, 2002, **10**, 4005-4012.
124. J. Wang, S. Dong, Y. Wang, Q. Lu, H. Zhong, G. Du, L. Zhang and Y. Cheng, *Bioorg. Med. Chem.*, 2008, **16**, 8510-8515.